Chironomid-inferred summer temperature during the Last Glacial Maximum in the Southern Black Forest, Central Europe

Pierre Lapellegerie, Laurent Millet, Damien Rius, Fanny Duprat-Oualid, Tomi Luoto, Oliver Heiri

Quaternary Science Reviews 345 (2024) 109016

Contents lists available at ScienceDirect

Quaternary Science Reviews

journal homepage: www.elsevier.com/locate/quascirev

Chironomid-inferred summer temperature during the Last Glacial Maximum in the Southern Black Forest, Central Europe

Pierre Lapellegerie [a,*], Laurent Millet [b], Damien Rius [b], Fanny Duprat-Oualid [b], Tomi Luoto [c], Oliver Heiri [a]

[a] Geoecology, Department of Environmental Sciences, University of Basel, Klingelbergstrasse 27, CH-4056, Basel, Switzerland
[b] CNRS UMR 6249, Laboratoire Chrono-Environnement, UFR des Sciences et Techniques, Université de Bourgogne-Franche-Comté, F-25000, Besançon, France
[c] Faculty of Biological and Environmental Sciences, Ecosystems and Environment Research Programme, University of Helsinki, Lahti, 15140, Finland

ARTICLE INFO

Handling editor: P Rioual

Keywords:
Quaternary
Palaeoclimatology
Palaeolimnology
Europe
Lake
Chironomidae
Last glacial maximum
July air temperature

ABSTRACT

The location of Bergsee (382 m a.s.l.), between the Black Forest and northern Alpine glaciers during their maximum extent of the Würm glaciation, makes the sediment record of this lake a unique palaeoenvironmental archive that probably recorded the entire Last Glacial Period. Here we present a chironomid record from Bergsee covering ca. 35 thousands of years (kyr) including the period corresponding to the Last Glacial Maximum in the northern Alpine area. The record is divided into 6 biostratigraphical zones. Between ca. 45.4–30.1 thousand calibrated ^{14}C years (cal ka BP) taxa typical for the littoral of relatively warm lakes (*Parakiefferiella bathophila*-type and *Paratanytarsus penicillatus*-type) are dominating. Then (ca. 30.1–23.3 cal ka BP), *Sergentia coracina*-type, a profundal and cold indicative taxon, becomes dominant alongside *Parakiefferiella bathophila*-type. Low diversity and high abundances of *Sergentia coracina*-type suggest the most severe environmental conditions of the record. The third zone (ca. 23.3–20.6 cal ka BP) is largely dominated by *Parakiefferiella bathophila*-type and warmer indicative taxa replace *Sergentia coracina*-type. In the fourth zone (ca. 20.6–16.9 cal ka BP), *Paratanytarsus penicillatus*-type and *Tanytarsus pallidicornis*-type dominate and the presence of *Chironomus anthracinus*-type suggests slightly warmer conditions, more nutrients or organic matter and lower oxygen availability in the lake. In the next zone (ca. 16.9–10.7 cal ka BP), *Corynocera ambigua*, a taxon with uncertain distribution in respect to temperature, becomes the dominant chironomid. Changing abundances of *Corynocera ambigua* match the climate variability of the Lateglacial, with high abundances corresponding to the cold phases of the Oldest and Younger Dryas interrupted by the warmer Bølling/Allerød interstadial. However, the high abundances of *Corynocera ambigua* are not necessarily due to colder temperature but could also be explained by changes in the trophic conditions in the lake or other environmental changes. The last zone (ca. 10.7–8.4 cal ka BP, onset of the Holocene), shows the highest diversity and presence of warm indicative taxa such as *Endochironomus tendens*-type and *Polypedilum nubeculosum*-type. The high abundances of *Corynocera ambigua* make the temperature reconstruction challenging for the Lateglacial since this taxon is restricted to cold lakes in some European chironomid-temperature calibration datasets, whereas it is known that it can also be found in high abundances in warmer lakes in other calibration datasets. A chironomid-temperature transfer function based on a Swiss-Norwegian calibration dataset reconstructed exceptionally cold values in the interval with maximum abundances of *Corynocera ambigua*, which disagree with reconstructions from other palaeoenvironmental archives in the region. To address this problem, the Swiss-Norwegian model was also used excluding *Corynocera ambigua* and another calibration dataset (Finnish), having a more realistic temperature optimum for *Corynocera ambigua*, was applied to the Bergsee chironomid record to evaluate the results. The reconstructions with the Swiss-Norwegian calibration dataset excluding *Corynocera ambigua* and with the Finnish calibration dataset resulted in a more realistic temperature development for the Lateglacial at Bergsee. The reconstructions based on these datasets indicate temperatures of ca. 11.6 °C for the period 45–30.1 cal ka BP, the coldest phase between 30.1 and 23.3 cal ka BP with July air temperature of ca. 10.5 °C, an abrupt warming at the beginning of the Bølling interstadial to ca. 16 °C and a decrease to 12.2 °C during the Younger Dryas. Another warming of 3.7 °C is estimated after the Younger Dryas and reconstructed temperatures reached ca. 16.4 °C in the Early Holocene. However, inferred

* Corresponding author.
E-mail address: pierre.lapellegerie@unibas.ch (P. Lapellegerie).

https://doi.org/10.1016/j.quascirev.2024.109016
Received 19 July 2024; Received in revised form 18 October 2024; Accepted 18 October 2024

temperatures in this range may already have been affected by the edge effect that can lead to underestimated temperatures close to the maximum temperatures covered by calibration datasets. The timing of the coldest phase is consistent with reconstructions of the expansion and maximum extent of northern Alpine glaciers, the pollen record from Bergsee and other palaeoenvironmental records in the region.

1. Introduction

The Last Glacial Period, dated to 115,000–11,700 years before present (115–11.7 ka BP), began after the Eemian interglacial (Shackleton et al., 2003) and ended with the beginning of the Holocene. In marine records, the period covers the interval from the Marine Isotope Stage (MIS) 5d to the oldest part of the MIS 1 (Lisiecki and Raymo, 2005) whereas over the continents it was characterised by several phases of glacier advances (Hughes et al., 2013) as well as abrupt changes in the climate affecting terrestrial and aquatic ecosystems (e.g., Guiot et al., 1989; Ampel et al., 2010; Harrison and Sánchez Goñi, 2010; Galbraith and Skinner, 2020; Bolland et al., 2021). In the North Atlantic, the period was marked by a multi-millennial-scale decrease in temperature towards the Last Glacial Maximum (LGM; Martrat et al., 2004; Sánchez Goñi et al., 2008), followed by a reversal towards warmer temperatures (Shakun and Carlson, 2010). In addition, as many as 26 stadial-interstadial cycles, showing centennial to millennial-scale variations, described based on shorter-term variations in oxygen isotope composition in Greenland ice cores, were superimposed on these long-term trends (Dansgaard et al., 1993; Rasmussen et al., 2014). Rapid warming episodes in Greenland, commonly referred to as Dansgaard-Oeschger events, were followed by gradual cooling (Grootes et al., 1993) with some of the cold stadials characterised by massive iceberg release in the North Atlantic, known as Heinrich events (Broecker et al., 1992; Bond et al., 1992). On the European continent, these climatic variations have been documented through, for example, vegetation changes (e.g., Müller et al., 2003; Fletcher et al., 2010; Pini et al., 2010) or oxygen isotope analyses in speleothems (e.g., Moseley et al., 2020). In southwestern sectors of Central Europe, the Last Glacial Period is referred to as the Würmian glaciation (Chaline and Jerz, 1984; Ivy-Ochs et al., 2008) and has been documented in various environmental archives (de Beaulieu and Reille, 1992; Antoine et al., 2013; Luetscher et al., 2015).

In the northern Alpine and pre-Alpine area, three major glacier advances have been documented for the Würmian glaciation with the latest one having the maximum extent (Ivy-Ochs et al., 2008) and roughly corresponding to the global maximum extent of glaciers between 26.5 and 19 ka BP (Clark et al., 2009). During these advances, ice sheets extended far into the Swiss Plateau through different glacier fronts (Ivy-Ochs et al., 2008; Preusser et al., 2011). Ice sheets also developed over the Vosges mountains (Mercier and Jeser, 2004) and the Black Forest (Hemmerle et al., 2016; Hofmann, 2023) but the synchronicity of the maximum extent of ice in these different regions remains unknown (Hofmann et al., 2020). The start of the deglaciation, which began around 19 ka BP in the Alps (Ivy-Ochs et al., 2004; Ivy-Ochs, 2015), occurred during a period of increasing Northern hemisphere summer insolation (Clark et al., 2009). Various proxy-based reconstructions covering sections of the last glaciation in Central Europe are available and provide information on past temperature variability (e.g., pollen records, $\delta^{18}O$ records of speleothems, studies of aquatic invertebrate remains; Guiot et al., 1993; Moseley et al., 2020; Bolland et al., 2021). However, many of these studies do not cover the LGM. This is particularly true for the northern pre-Alpine forelands (e.g., Heiri et al., 2014), where quantitative palaeotemperature reconstructions covering the LGM are largely lacking. Nevertheless, studies on speleothems providing information on past precipitation and wind patterns (e.g., Luetscher et al., 2015; Spötl et al., 2021), as well as climate simulations providing model-based estimates of past temperature (e.g., Kim et al., 2003; Russo et al., 2024) are available for the LGM in the Alpine region. Very few palaeolimnological investigations have been developed for this period, since most lake basins were either covered with ice or not formed yet (Duprat-Oualid et al., 2017; Rey et al., 2020).

Chironomids, also known as non-biting midges, are widely distributed and abundant in freshwater environments (Armitage et al., 1995). Summer temperature plays an important role in the geographical distribution of chironomid species throughout the world and affects metabolic processes as well as growth and development of the different stages of their life cycle (Walker et al., 1991; Eggermont and Heiri, 2012). Subfossil remains of the larval stages preserve well and are usually abundant in Quaternary lake sediments allowing palaeolimnologists to identify them at generic or morphotype levels (Brooks et al., 2007). Therefore, the former distribution and abundance of chironomid larvae in lakes can be reconstructed, providing a way to constrain past temperature variations from chironomid remains in lake sediment records. Calibration datasets describing the distribution of chironomid morphotypes over large spatial and temperature gradients have been developed for different regions of the world (e.g., Walker et al., 1997; Eggermont et al., 2010; Heiri et al., 2011). Numerical inference models (transfer functions) developed from these calibration datasets can in turn be used to quantitatively reconstruct past summer air temperature based on the subfossil chironomids identified in lake sediments. Chironomid-based temperature reconstruction has been widely used to constrain past summer temperature variability during the Würmian Lateglacial (e.g., Brooks, 2000; Millet et al., 2012; Samartin et al., 2012; Bolland et al., 2020). Earlier intervals have received much less attention, but several chironomid-based temperature reconstructions are now available for different periods from the Early to the Late Würmian (Engels et al., 2008, 2010; Bolland et al., 2021, 2022; Ilyashuk et al., 2022). However, very few reconstructions covering the global LGM and the phase of maximum ice extent in the European Alps are available (ca. 26.5–21 ka BP; Ivy-Ochs et al., 2004; Monegato et al., 2007). To our knowledge, the only available chironomid-based temperature reconstruction covering the LGM is from the southern forelands of the Alps (Samartin et al., 2016), with only very limited quantitative information on past temperature variability based on other proxy-types (Heiri et al., 2014). Therefore, there is an urgent need for more quantitative temperature reconstructions to fill the gap of knowledge on temperature changes during this period. This is particularly relevant since the LGM can be expected to encompass some of the coldest and therefore most limiting environmental conditions of the Würmian glaciation for the local survival of both terrestrial and aquatic organisms in the Alps and their forelands.

The aim of this study is to develop a new chironomid record from Bergsee, a small lake on the southern fringe of the Black Forest, Germany. The lake's basin was formed well before the northern Alpine LGM and therefore includes the full sequence of sediments deposited immediately prior to, during, and after the maximum glacier extent in the Alps and the Black Forest. Based on the new chironomid record we aim to develop a quantitative summer air temperature reconstruction covering the LGM in the southwestern sector of Central Europe. By doing so, we hope to provide a new, well dated palaeotemperature record that will be available for a potential user community that could include glaciologists, aiming to determine drivers and dynamics of the late Würmian glacial advances and retreats, but also archaeologists and palaeoecologists, interested in understanding climate conditions in this crucial and understudied phase of the latest Pleistocene climate history.

2. Materials and methods

2.1. Study site

Bergsee is a small eutrophic lake, 335 m long and 250 m wide, located on the Southern piedmont of the Black Forest in southern Germany (47°34′16″N, 7°56′6″E; 382 m a.s.l.; Fig. 1). The water level was artificially raised by the building of a dam in the 19th century by about 6 m, to reach 13 m maximum depth today (Müller, 1994). The lake has no natural inlets and therefore was only fed by precipitation, groundwater inflow and the natural run-off from its small natural catchment (0.162 km^2) before the channelisation of several streams (Becker et al., 2006). A topographic map of the Black Forest as well as a bathymetric map of Bergsee are available in Duprat-Oualid et al. (2017). The limnology of Bergsee has been studied in detail during the 20th and 21st centuries (e.g., Wütrich and Leser, 2000), however, due to the hydrological modifications and artificial aeration these assessments can not be considered as representative for the natural conditions of the lake. The bedrock surrounding Bergsee is, like the rest of the Black Forest, mainly composed of gneiss and granite (Becker et al., 2004). Bergsee is part of a former subglacial channel system that probably formed during the Riss glaciation when the Rhine glacier reached the area (Geyer et al., 2003; Becker and Angelstein, 2004). During the Würmian LGM, the lake was not covered by glaciers, due to its position between the Black Forest glacier to the north and the Rhine glacier to the south making it a unique environmental archive that probably recorded the entire Last Glacial period (Becker et al., 2006). The lake was historically named "Schwarzsee" (Black Lake) suggesting humic conditions before the recent modifications (Becker et al., 2006). Considering the maximum depth of the lake before the building of the dam (6 m) and the length of the sediment core extracted (28.5 m, see Section 2.2), it is clear that Bergsee was considerably deeper in the past. However, due to uncertain effects of sediment compaction and possible changes in outlets it is not possible to obtain reliable palaeodepth estimates. Over the past ten years, the mean July air temperature at Bergsee is estimated to have been around 19.9 and 20.7 °C based on the measurements of Möhlin (343 m a.s.l.) and Basel/Binningen (316 m a.s.l) weather stations (MeteoSwiss) adjusted for elevation differences following Livingstone et al. (1999).

Previous studies have examined pollen (Duprat-Oualid et al., 2017) and geochemistry (Kämpf et al., 2022) in Bergsee sediment cores for the period analysed in the present study. Between 45 and 30 thousand calibrated ^{14}C years BP (cal ka BP), the vegetation around the lake repeatedly changed between steppe and boreal forest (Duprat-Oualid et al., 2017). Between 30 and 23.5 cal ka BP the vegetation around the lake was an *Artemisia* dominated steppe indicating cold and dry climate (Duprat-Oualid et al., 2017). Finally, between 23.5 and 14.7 cal ka BP the presence of *Betula* pollen, although in low abundances, indicates more humid conditions after the LGM (Duprat-Oualid et al., 2017). An earlier chironomid record is available from Bergsee but with a lower taxonomic and temporal resolution than the present study and only dated by one ^{14}C date for the period older than 12,000 ^{14}C years BP (Becker et al., 2006). It was therefore not possible to develop a detailed chironomid-based temperature reconstruction from this record.

2.2. Coring and chronology

Bergsee was cored in 2013 in its centre, at 11 m water depth. From the retrieved sediment cores, a 28.26 m long master core was built using magnetic susceptibility and high-resolution core imaging. Detailed descriptions of the sediments, grain size analyses, mineralogic assessments, total organic and inorganic carbon as well as C/N ratios are given in Kämpf et al. (2022). The sediment record analysed in the present paper is divided as follows: light brownish to grey sediments with low TOC (28.26–16.1 m), a transitory laminated sediment (16.1–14.5 m) and a dark brownish organic mud with high TOC and C/N values (14.5–13.7 m; Kämpf et al., 2022). More information on the coring, core correlation and sediment geochemistry are provided in Duprat-Oualid (2019) and Kämpf et al. (2022).

The age-depth model for Bergsee presented by Duprat-Oualid et al. (2017) was later updated with 6 new ^{14}C dates (Kämpf et al., 2022 and data in the Supplementary online information). The IntCal 20 calibration curve (Reimer et al., 2020) and the clam version 2.5.0 (Blaauw et al., 2022) package in R studio version 2023.09.1 (R Core Team, 2022) were used to develop a revised age-depth model for the sediment record based on a smooth spline (degree of smoothing: 0.3) and 10,000

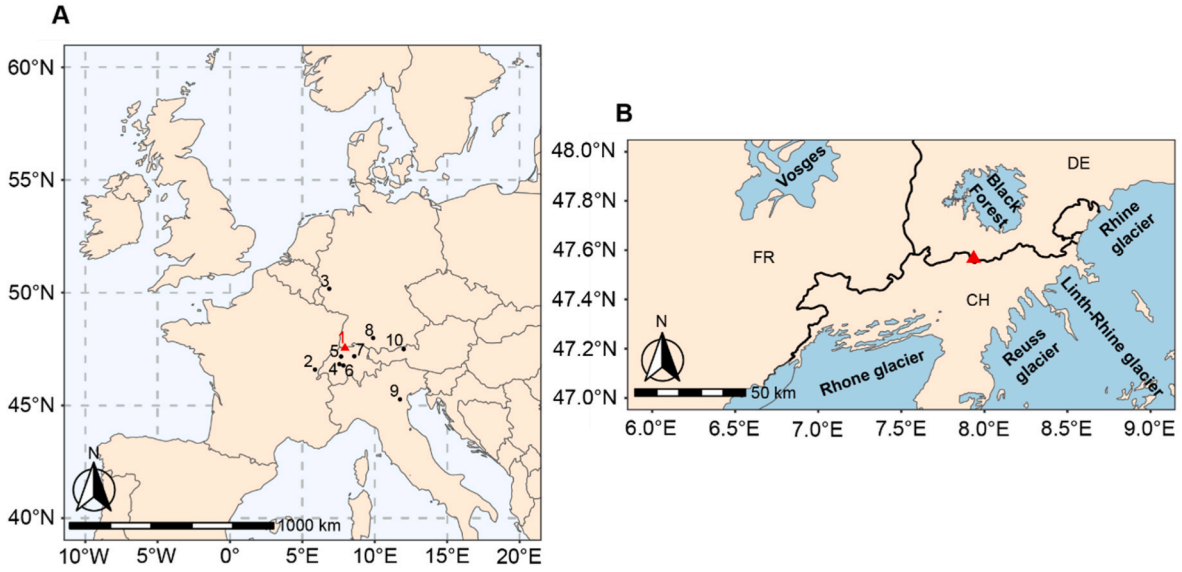

Fig. 1. A: Location map showing Bergsee and other sites discussed in the text: 1. Bergsee (Becker et al., 2006; Duprat-Oualid et al., 2017; Kämpf et al., 2022; this study), 2. Lac Lautrey (Heiri and Millet, 2005), 3. Eiffel volcanic field (Zander et al., 2024), 4. Gerzensee (Brooks, 2000; Lotter et al., 2012), 5. Burgäschisee (Bolland et al., 2020), 6. Sieben Hengste (Luetscher et al., 2015), 7. Egelsee (Larocque-Tobler et al., 2010), 8. Füramoos (Bolland et al., 2021), 9. Lago della Costa (Samartin et al., 2016), 10. Unterangerberg (Ilyashuk et al., 2022). B: Location of Bergsee (red triangle) and the assumed Würmian maximum ice extent (LGM) in the Black Forest (Hemmerle et al., 2016), the Vosges and Switzerland (Ehlers et al., 2011). CH: Switzerland, DE: Germany, FR: France. Data from the package rnaturalearth version 1.0.1 (Massicotte and South, 2023) were used to make the maps in R studio version 2023.09.1 (R Core Team, 2022).

iterations to infer sediment ages and uncertainties.

2.3. Chironomid and aquatic invertebrate analysis

A total of 134 4-cm-thick samples, with a volume ranging from 2 to 5 cm^3, were analysed for chironomids and other aquatic invertebrates. The samples were taken on the same cores as the pollen samples from Duprat-Oualid et al. (2017) and geochemical analyses of Kämpf et al. (2022). No chemical treatment was required so the samples were simply sieved gently under water through a 100 μm sieve (Brooks et al., 2007). Chironomid head capsules as well as other chitinous aquatic remains (e.g., Cladocera ephippia, insect mandibles) were hand-picked from the sieved residue using a Bogorov tray (Gannon, 1971) under a stereomicroscope (20–50× magnification) before being permanently mounted using Euparal. Chironomids were identified using Wiederholm (1983), Schmid (1993) and Brooks et al. (2007) under a compound microscope (100–400× magnification). Head capsules with more than half a mentum were counted as one, head capsules with half a mentum were counted as half and head capsules with less than half mentum were not counted. For *Paratanytarsus*, the mandibles were rarely preserved making the identification to morphotype level challenging. However, the vast majority of specimens with mandibles belonged to *Paratanytarsus penicillatus*-type, therefore the specimens lacking mandibles were assigned to this morphotype. For the head capsules belonging to the *Tanytarsus* genus, those missing mandibles were assigned to *Tanytarsus* morphotypes based on the proportions of the identified specimens with mandibles (e.g., Bolland et al., 2021).

Cladoceran ephippia of daphniids were identified using Vandekerkhove et al. (2004) and Szeroczyńska and Sarmaja-Korjonen (2007), insect mandibles based on a slide collection at the University of Basel partly published in Courtney-Mustaphi et al. (2024), bryozoan statoblasts with Wood and Okamura (2005) and oribatid mites with Solhøy and Solhøy (2000). *Chaoborus* mandibles and thoracic horns were identified with Uutala (1990) and Salmela et al. (2021) and the minimum number of individuals per sample was estimated based on these two remains. Oogonia produced by charophytes were enumerated and identified using Haas (1994).

2.4. Statistical analyses

A minimum count of 50 head capsules was aimed for in each sample (Heiri and Lotter, 2001; Larocque, 2001; Quinlan and Smol, 2001a). However, some adjacent samples needed to be grouped together to reach this count sum for statistical analyses resulting in 84 samples with a minimum count of 51 head capsules (mean: 105). As described below, we also explored reconstructions excluding *Corynocera ambigua* and since this taxon was very abundant in some samples, removing it resulted in three samples with effective counts between 33 and 45 head capsules (14.685, 15.570 and 16.045 m). Subsequent analyses were all performed on square root transformed percentage data unless specified otherwise.

2.4.1. Zonation and ordination

Zones in the chironomid record were assessed by the constrained cluster algorithm CONISS (Grimm, 1987) with Euclidean distance as distance measure. A broken stick model (Bennett, 1996) was used to determine the number of statistically significant zones. Analyses were performed with the rioja package version 1.0–6 (Juggins, 2023) in R Studio version 2023.09.1 (R Core Team, 2022).

Major changes in the chironomid assemblages were summarized with a Detrended Correspondence Analysis (DCA) performed with CANOCO 5.11 (Šmilauer and Lepš, 2014).

2.4.2. Diversity

Alpha diversity was calculated for the chironomid assemblages using rarefaction which estimates the taxon richness for each sample using a fixed count size (i.e., based on the smallest count sum among our samples of 51; Birks and Line, 1992). This rarefaction was calculated on untransformed count data using the function 'rarefy' of the vegan package version 2.6–4 (Oksanen et al., 2022) in R Studio version 2023.09.1 (R Core Team, 2022).

2.4.3. Temperature reconstructions

Several chironomid-based temperature reconstructions were produced using different modern calibration datasets documenting the distribution of chironomid taxa in regard to July air temperature. Models were calculated based on a Swiss-Norwegian calibration dataset that has been extensively used in Central Europe and the Alpine region (Heiri et al., 2011) as well as on a Finnish calibration dataset (Luoto et al., 2014) that was considered to contain a more realistic distribution of *Corynocera ambigua*, one of the key taxa in the Bergsee record. Morphotypes that were not included in the modern calibration datasets but identified in the Bergsee record were excluded when performing the reconstructions. Inference models developed from these calibration datasets were based on Weighted Averaging Partial Least Squares (WA-PLS) regression (ter Braak et al., 1993) with two components and used to estimate past mean July air temperatures from fossil assemblages. Cross-validated performance and error statistics of each model were calculated based on bootstrapping with 9999 bootstrap cycles. The respective characteristics of the different models are shown in Table 1.

Squared chi-square distances were calculated to identify fossil assemblages with either "no close" or "no good" modern analogues in the modern calibration datasets (Birks et al., 1990), with respective thresholds set as the 2nd and 5th percentiles of all distances within the modern calibration datasets (Birks et al., 1990). Furthermore, a Canonical Correspondence Analysis (CCA) of the different calibration datasets, with mean July air temperature as the only constraining variable, was produced with the fossil samples added passively. The 90th and 95th percentiles of residual distances of the samples of the modern calibration datasets to axis 1 were used to determine fossil samples with a "poor" and "very poor" goodness-of-fit to temperature, respectively (Birks et al., 1990). In addition, the number of rare taxa ($N_2 < 5$ in the calibration datasets) in each sample (Heiri et al., 2003) as well as the percentage of taxa absent in the calibration datasets were calculated. C2 version 1.7.7 (Juggins, 2017) was used to calculate the temperature

Table 1
Descriptive statistics of the different WA-PLS inference models and calibration datasets used in this paper. Performance and error statistics (r^2, RMSEP, maximum bias and average bias) for the WA-PLS models are based on bootstrapping with 9999 bootstrap cycles. The number (Nb.) of fossil samples with close, good and no good analogues are based on the distances of the fossil samples to the most similar samples in the calibration datasets as assessed with MAT models. Asterisks indicate whether the components of the WA-PLS models are significant at the p = 0.01 level.

	Swiss-Norwegian	Swiss-Norwegian, *C. ambigua* excluded	Finnish
Sites	255	255	139
Taxa	151	150	117
July air temperature (°C)	3.5–18.4	3.5–18.4	7.9–17.1
Numerical approach	WA-PLS	WA-PLS	WA-PLS
r^2	0.87	0.87	0.88
RMSEP (°C)	1.40	1.43	0.88
% change component 1 to 2	17.3**	17.0**	19.7**
% change component 2 to 3	−0.7	0.08	−1.0
Maximum bias (°C)	0.97	1.04	1.18
Average bias (°C)	−0.02	−0.03	0.00
Numerical method for analogue detection	MAT	MAT	MAT
Nb. close analogues	12	12	0
Nb. good analogues	52	47	2
Nb. no good analogues	20	25	82

reconstructions and analogue statistics. CANOCO 5.11 (Šmilauer and Lepš, 2014) was used to perform the CCA.

3. Results

3.1. Chironomid and aquatic invertebrate record

A total of 8860 chironomids from 80 different morphotypes were identified in the samples from Bergsee. In addition, a few other aquatic invertebrate remains from cladocerans, insects, bryozoans and oribatid mites were isolated from the sediment and enumerated (Fig. 2). CONISS and broken stick model analyses identified 6 statistically significant zones in the chironomid record (BER-1 to BER-6). Overall, chironomid head capsules are the most abundant aquatic invertebrate remains throughout the record with *Daphnia* ephippia being relatively abundant in the oldest sections and Ephemeroptera and *Chaoborus* mandibles increasing in the youngest sections. Oogonia were found throughout the record.

The aquatic invertebrate assemblages of BER-1 (45.4–30.1 cal ka BP) were dominated by chironomids and *Daphnia* ephippia until 35.6 cal ka BP. After that, the relative abundances of *Daphnia* decreased. *Chaoborus* and Sialidae were present in rather low abundances during the zone. The chironomid assemblages were relatively diversified in this zone (median rarefaction value: 10) and several taxa were present in relatively high abundances. *Paratanytarsus penicillatus*-type and *Parakiefferiella bathophila*-type dominated the chironomid fauna with *Tanytarsus lugens*-type, whereas *Procladius* and *Tanytarsus pallidicornis*-type were subdominant.

During BER-2 (30.1–23.3 cal ka BP) the diversity of the chironomid assemblages drastically decreased (median rarefaction value: 3.6) and *Sergentia coracina*-type became a dominant taxon together with *Parakiefferiella bathophila*-type. These two taxa often composed more than 80% of the chironomid assemblages in this section of the record. The dominant taxon alternated between these two morphotypes a few times throughout the zone. *Tanytarsus lugens*-type and *Paratanytarsus penicillatus*-type were the only other taxa to reach a relative abundance of 10%. *Daphnia* ephippia were still present throughout the zone but stayed in low relative abundances and *Chaoborus* were only present between 27.1 and 24.3 cal ka BP.

BER-3 (23.3–20.6 cal ka BP) was first dominated by *Parakiefferiella bathophila*-type until 21.5 cal ka BP, which accounted for as much as 80% of the chironomid assemblages. Then, *Tanytarsus pallidicornis*-type became the dominant chironomid for the rest of the zone. The diversity of the chironomid assemblages in this zone increased (median rarefaction value: 6.4) but stayed lower than during BER-1. *Daphnia* was the only other aquatic invertebrate detected in this zone.

BER-4 (20.6–16.9 cal ka BP) was dominated by *Paratanytarsus penicillatus*-type and *Tanytarsus pallidicornis*-type. *Parakiefferiella bathophila*-type continued to decrease to reach its lowest relative abundance since the beginning of the record and the diversity of the chironomid assemblages stabilised (median rarefaction value: 6.9). *Cricotopus intersectus*-type and *Corynoneura arctica*-type were joined by *Chironomus anthracinus*-type as subdominant taxa.

In BER-5 (16.9–10.7 cal ka BP) *Corynocera ambigua* appeared for the first time and became the dominant chironomid during two periods (16.7–14.2 and 12.4–11.2 cal ka BP). The diversity of the chironomid assemblages increased (median rarefaction value: 8.3) to reach similar values as in BER-1. *Tanytarsus glabrescens*-type, *Tanytarsus pallidicornis*-type and *Ablabesmyia* increased in relative abundances, together with the diversity, when *Corynocera ambigua* decreased between 14.2 and 12.4 cal ka BP. *Plumatella* and Oribatida were also increasing during this interval while relative abundances of chironomids in the invertebrate assemblages decreased.

BER-6 (10.7–8.4 cal ka BP) was dominated by *Microtendipes pedellus*-type, *Glyptotendipes pallens*-type and *Endochironomus tendens*-type. The relative abundances of *Tanytarsus pallidicornis*-type, *Tanytarsus mendax*-type and *Procladius* increased during this zone. The diversity of the chironomid assemblages reached its highest values of the record (median rarefaction value: 17.9). Overall, the relative abundances of chironomids decreased whereas *Chaoborus*, Ephemeroptera and *Daphnia* all increased.

3.2. Chironomid-inferred temperature reconstructions

Three chironomid-inferred July air temperature reconstructions based on two different calibration datasets have been calculated with their respective diagnostic statistics (Fig. 3). Initially, a reconstruction based on the Swiss-Norwegian calibration dataset was calculated following Heiri et al. (2011). A preliminary examination of the results indicated that one taxon, *Corynocera ambigua*, had a disproportionate effect on the results, since it is restricted to cool lakes in the Norwegian dataset, in contrast to other published calibration datasets (e.g., Luoto et al., 2014; Nazarova et al., 2015) demonstrating that the taxon can also colonise relatively warm lakes. This led to unrealistic reconstructed values in the uppermost section of the record (see Discussion, below). Therefore, a second reconstruction was calculated based on the Swiss-Norwegian calibration dataset with *Corynocera ambigua* excluded from the calibration and fossil datasets. To assess whether this reconstruction provided realistic values that could also be supported by an independent reconstruction, we also used a two-component WA-PLS model based on the Finnish calibration dataset (Luoto et al., 2014) in which *Corynocera ambigua* has a wider distribution in regard to temperature than in the Swiss-Norwegian calibration dataset.

Overall, the two reconstructions based on the Swiss-Norwegian calibration dataset are very similar with the exception of BER-5 where *Corynocera ambigua* is abundant. In the oldest section (BER-1; 45.4–30.1 cal ka BP) the reconstructions give values fluctuating between 9.8 and 13.7 °C (mean July air temperature: 11.6 °C) with three rapid increases in July air temperature at 41, 38.5 and 33 cal ka BP. During BER-2 (30.1–23.3 cal ka BP), the reconstructed July air temperature appears colder and more stable (mean July air temperature: 10.5 °C). BER-3 (23.3–20.6 cal ka BP) starts with a sharp increase of temperature which then stays stable during the zone (mean July air temperature: 12.4 °C). During BER-4 (20.6–16.9 cal ka BP), the temperatures reconstructed for most of the samples are stable (mean July air temperature: 12.3 °C) with the exception of the sample at 19.2 cal ka BP which has a much colder reconstructed temperature (10.8 °C) caused by the presence of *Micropsectra radialis*-type. In BER-5 (16.9–10.7 cal ka BP), the temperature reconstructed is highly variable in the two scenarios varying from 7.6 to 16.4 °C with the default model based on the Swiss-Norwegian calibration dataset and from 11.2 to 16.5 °C with the model where *Corynocera ambigua* is excluded. In both scenarios, the warmest period of the zone is between 14.5 and 13.6 cal ka BP. Finally, in BER-6 (10.7–8.4 cal ka BP), the July air temperature sharply increases to 16 °C in both scenarios.

The reconstruction calculated with the Finnish calibration dataset is similar to the two reconstructions based on the Swiss-Norwegian calibration dataset for most of the record, but seems to often give slightly warmer temperatures. This is particularly true for BER-3 (23.3–20.6 cal ka BP), where the Finnish reconstruction estimated summer air temperature around 14.7 °C whereas the reconstructions with the Swiss-Norwegian calibration dataset estimated 12.3 °C. During BER-5, which includes the Lateglacial and parts of the Early Holocene (16.9–10.7 cal ka BP), the reconstructed temperatures are very similar to those calculated with the Swiss-Norwegian calibration dataset where *Corynocera ambigua* was excluded for the oldest peak of abundances of this taxon (16.7–14.2 cal ka BP) but intermediate between the two models for the youngest peak (12.4–11.2 cal ka BP). Importantly, all the reconstructions support the minimum temperatures estimated by the transfer function based on the Swiss-Norwegian calibration dataset during the period 30.1–23.3 cal ka BP.

The Finnish model has the lowest cross-validated Root Mean Square

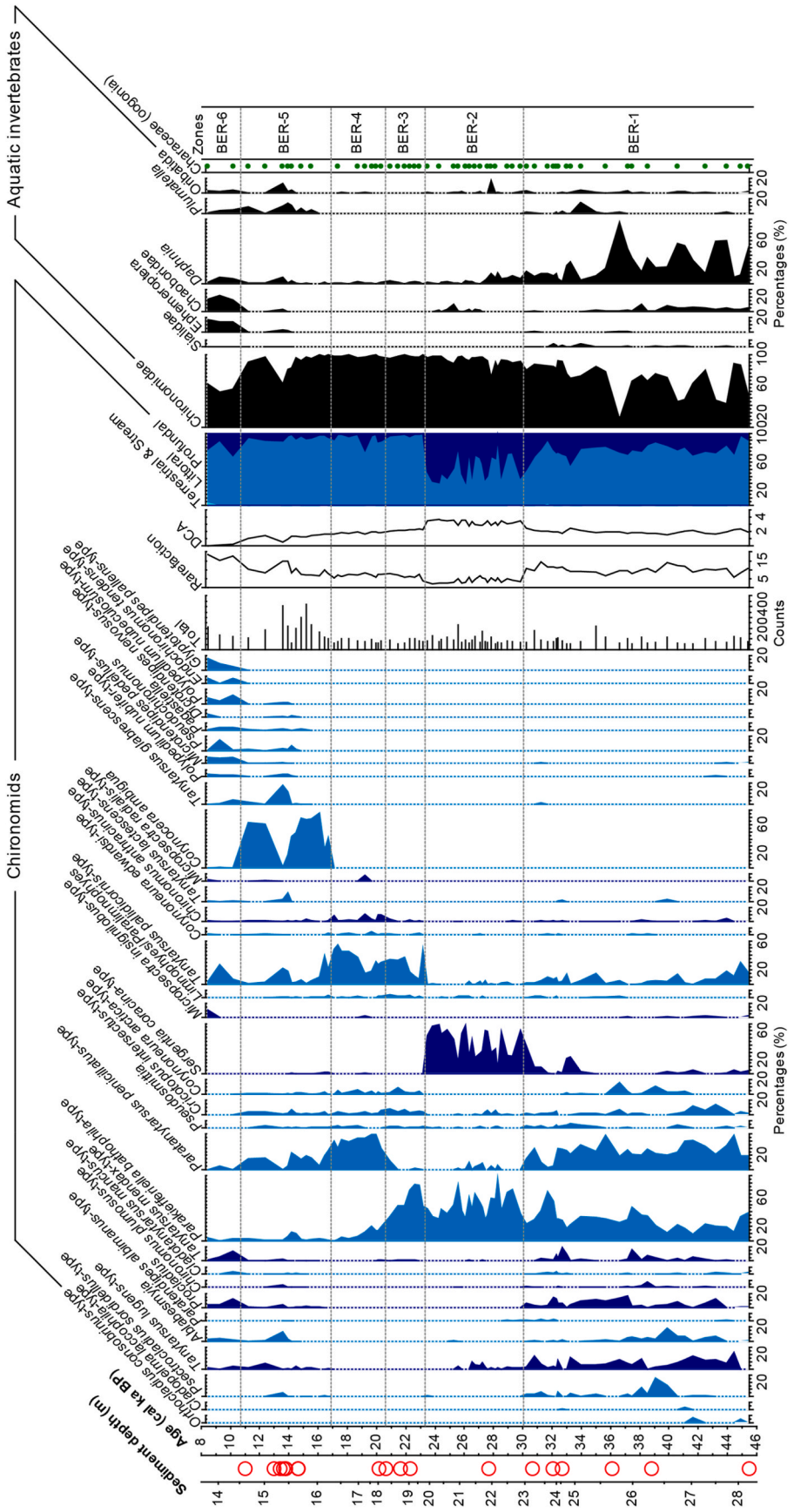

(caption on next page)

Fig. 2. Fossil chironomid and other aquatic invertebrate remains in the sediment of Bergsee. From left to right: depth scale, position of AMS ^{14}C dates (red circles), age scale, chironomid percentages of taxa with a cumulative abundance in the record >5% (littoral taxa in blue, profundal taxa in dark blue), total number of chironomids per sample, rarefaction of the chironomid assemblages, DCA axis 1 scores, percentage curves of taxa grouped by habitat preference (based on Sæther, 1979; Janecek et al., 2017), aquatic invertebrate percentages calculated following Ursenbacher et al. (2020), presence of oogonia in sediment sample (green dots) and significant zones calculated with the CONISS algorithm.

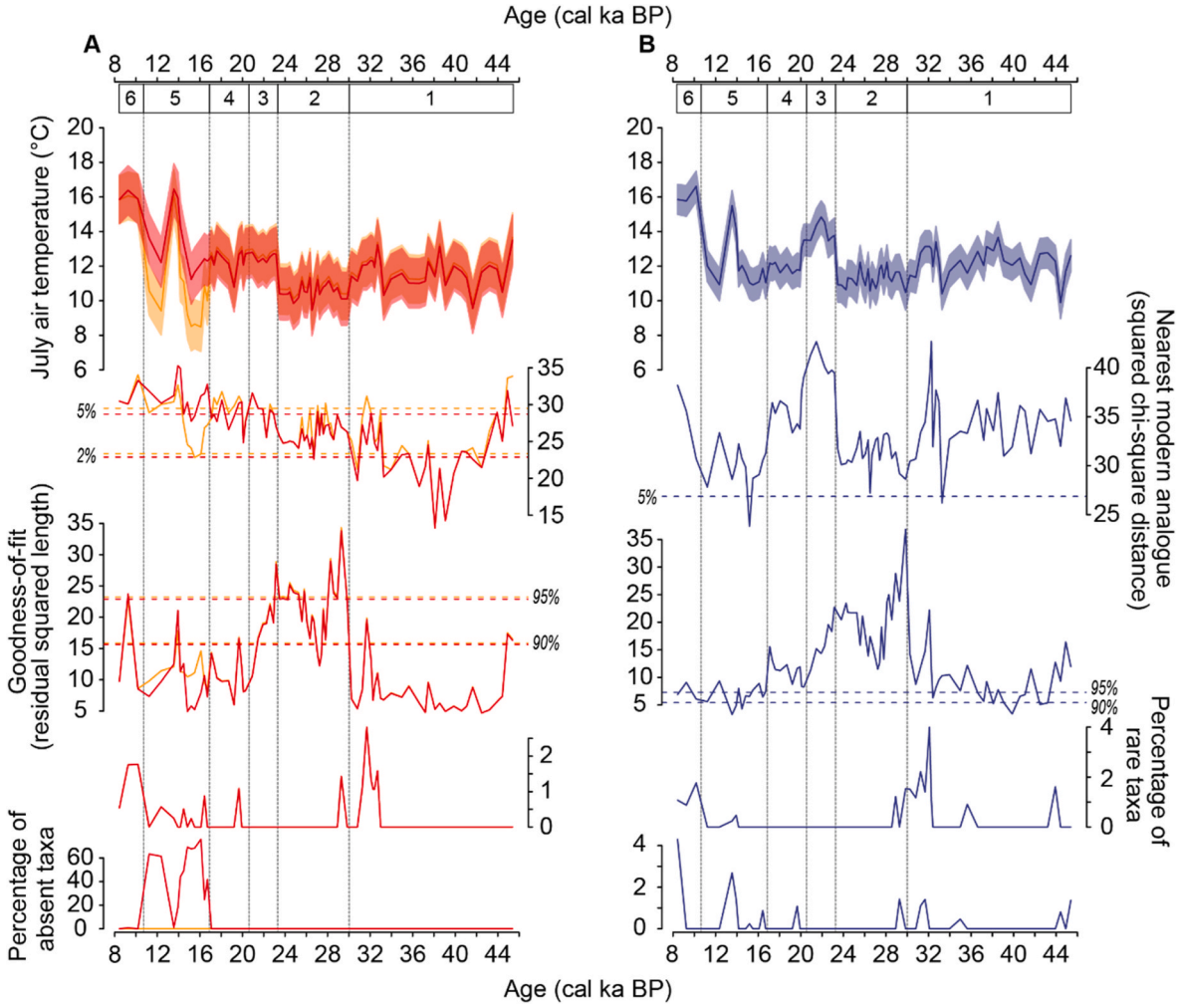

Fig. 3. Chironomid-inferred July air temperature calculated based on the Swiss-Norwegian calibration dataset (**A**) with *Corynocera ambigua* included (orange) and excluded (red) and based on the Finnish calibration dataset (**B;** blue) with their respective diagnostic statistics. From top to bottom: Chironomid-inferred July air temperature and associated error estimates; squared chi-square distance of fossil samples to the nearest modern analogue in the calibration datasets, the dashed lines indicate the thresholds for no close (2%) and no good (5%) analogues in the modern calibration datasets; residual squared length of the fossil samples to the first axis of a Canonical Correspondence Analysis (CCA) of the modern calibration dataset with mean July air temperature as only constraining variable, dashed lines indicate thresholds for poor fit (90%) and very poor fit (95%) with temperature; percentage of taxa in fossil samples that are rare in the calibration datasets; percentage of taxa in fossil samples absent in the calibration datasets.

Error of Prediction (RMSEP: 0.88 °C) followed by the Swiss-Norwegian models (1.40 and 1.43 °C, respectively for the default model and the model where *Corynocera ambigua* is excluded). Modern analogue statistics indicate that most of the samples in BER-1 and 2 have good analogues in the Swiss-Norwegian calibration dataset whereas this is much less the case in the other zones. The samples of the oldest peak in abundances of *Corynocera ambigua* (16.7–14.2 cal ka BP) have close analogues in the Swiss-Norwegian calibration dataset for the reconstruction with the default model, which is not the case with the other models. In contrast, only two fossil samples have good modern analogues in the Finnish calibration dataset. The temperature estimates calculated with the Swiss-Norwegian models have poor goodness-of-fit for most of the record with the exception of the samples in BER-2 which have mostly very poor goodness-of-fit. The residual squared length distance is also larger for the samples in BER-2 with the reconstructions calculated with the Finnish calibration dataset. In the Finnish reconstruction, most of the samples have poor goodness-of-fit with the exception of BER-2. Most of the samples have low percentages (< 4 %) of rare taxa in the modern calibration datasets.

4. Discussion

4.1. Chironomid and aquatic invertebrate assemblage changes

The Bergsee record shows pronounced changes in the chironomid assemblages, with major ones occurring at the transitions between BER-1 and 2 (ca. 30.1 cal ka BP) and between BER-2 and 3 (ca. 23.3 cal ka BP) as shown by the DCA analysis (Fig. 2). Another noticeable change

occurred at the well-described temperature transition at the beginning of the Bølling interstadial at ca. 14.7 cal ka BP (Ammann et al., 2013). This transition is dated slightly younger in the Bergsee sediment (ca. 14.1 cal ka BP) due to dating uncertainties but clearly constrained by the maximum in *Juniperus* pollen of the record, which is dated to ca. 14.6–14.5 in pollen records from the Swiss Plateau (Ammann et al., 2013; Rey et al., 2020, Fig. 4). In addition, distinct changes also occurred in the chironomid assemblages at the transitions into the Younger Dryas cold episode (ca. 12.9 cal ka BP; Shakun and Carlson, 2010) and into the Early Holocene (ca. 11.6 cal ka BP; Ammann et al., 2013). Chironomid assemblages were mainly dominated by taxa typical of shallow environments such as *Parakiefferiella bathophila*-type, *Tanytarsus pallidicornis*-type or *Paratanytarsus penicillatus*-type which can all be abundant in the littoral zone of lakes (Lods-Crozet and Lachavanne, 1994; Brodersen et al., 2001; Heiri, 2004; Janecek et al., 2017) and are usually found in temperate lowland to subalpine lakes (Luoto, 2009; Heiri et al., 2011; Nazarova et al., 2015). In contrast, several other taxa such as *Sergentia coracina*-type, *Tanytarsus lugens*-type and *Procladius* are common in deepwater habitats (Sæther, 1979; Janecek et al., 2017) but can also colonise the littoral zones under specific conditions (Hofmann, 2001; Heiri, 2004). For example, the cold stenotherms *Sergentia coracina*-type and *Tanytarsus lugens*-type can live in shallow environments under cold climate (Brundin, 1949; Brodin, 1986). Very few rheophilous taxa were found in the chironomid record of Bergsee indicating that the lake was not influenced by in-flowing waters and was probably without a major natural inlet as early as 45 ka ago (Becker et al., 2006).

BER-1 (45.4–30.1 cal ka BP) was dominated by chironomid taxa commonly living in the littoral zones of lowland to subalpine lakes such as *Parakiefferiella bathophila*-type and *Paratanytarsus penicillatus*-type (Heiri et al., 2011). Although *Parakiefferiella bathophila*-type is generally considered a littoral taxon it can also be found in the profundal zone of lakes (Brundin, 1949; Moller Pillot, 2013). This taxon seems to be more abundant in lakes with low to moderate nutrient concentration but can sometimes colonise nutrients-rich lakes (Moller Pillot, 2013). During this zone, *Parakiefferiella bathophila*-type was present in relatively high percentages (mean: 29 %), which is not the case in the different calibration datasets, where this taxon is usually commonly found only in rather low abundances (Heiri et al., 2011; Luoto et al., 2014; Nazarova et al., 2015). However high abundances of *Parakiefferiella bathophila*-type have been recorded in sediment cores from the Lateglacial in previous studies. For example, in a littoral core from Gerzensee, Switzerland, the taxon was present in high abundances (30–50 %) between 13.5 and 12.7 cal ka BP including the cold Gerzensee Oscillation (Brooks, 2000). In Lago della Costa, northern Italy, the taxon has been found in high abundances (more than 40 %) in sediment samples from 17 cal ka BP (Samartin et al., 2016). These findings suggest that this taxon, or at least one species of this morphotype, could have been more dominant in lakes in the past due to overall colder temperatures and was better adapted to these conditions, at least in some lakes. Species of *Paratanytarsus* are often associated with macrophytes (Lods-Crozet and Lachavanne, 1994; Čerba et al., 2010) and the relatively high abundances of this taxon in the zone may indicate a well-developed macrophyte belt. This interpretation is supported by the continuous presence of oogonia of Characeae in the sediment (Fig. 2). *Tanytarsus lugens*-type was present during almost the entire zone, suggesting summer stratification with cold bottom water or overall cold climatic conditions, and rather low nutrient concentrations (Brundin, 1949; Sæther, 1979). This summer stratification could be supported by the presence of *Chaoborus* until 35 cal ka BP which suggests rather low oxygen conditions at least during a short period during the summer (Quinlan and Smol, 2010; Ursenbacher et al., 2020). In this part of the record mandibles belonging to *Chaoborus flavicans*-type were present, a group particularly common in small lakes with low oxygen conditions when fish are present, as these insect larvae can migrate into the anoxic zone during the day to avoid predation by fish (Dawidowicz et al., 1990; Sweetman and Smol, 2006; Luoto and Nevalainen, 2009). In Bergsee, no fish remains have been identified so it is not possible to confirm their presence or absence. The presence of taxa typical of more nutrient-rich lakes such as *Tanytarsus mendax*-type, *Chironomus plumosus*-type and *Chironomus anthracinus*--type, even though in relatively low abundances, could indicate slightly

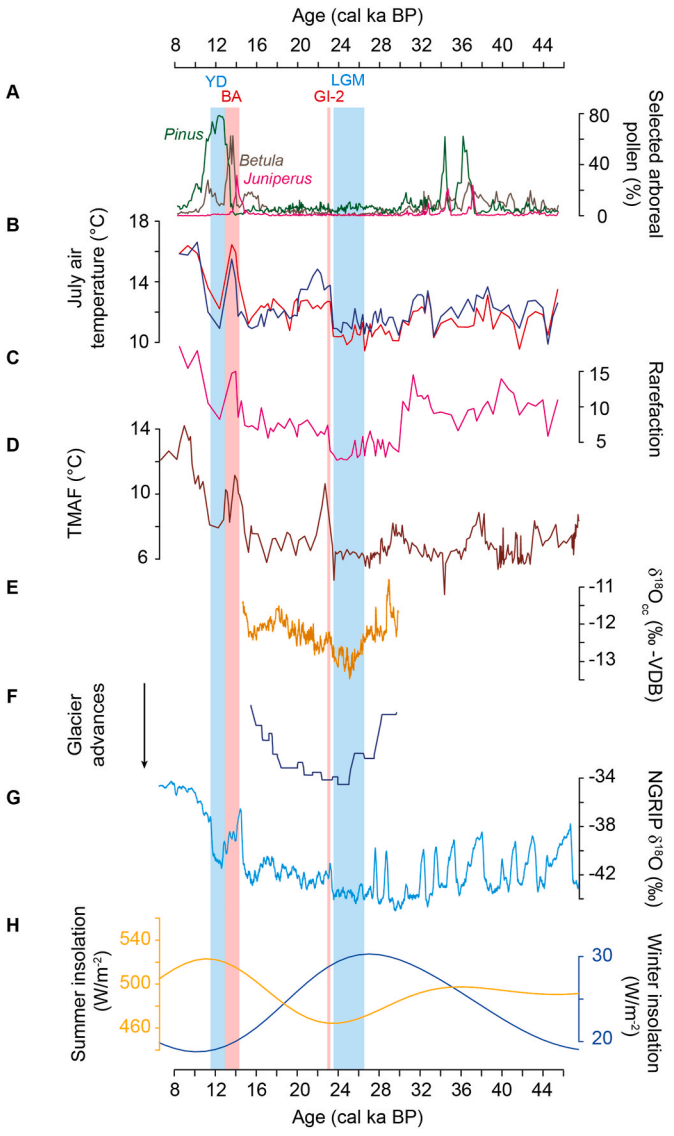

Fig. 4. Chironomid-inferred summer air temperature from Bergsee compared to other palaeoenvironmental and palaeoclimate records. From top to bottom: A. Selected tree and shrub pollen for Bergsee: *Juniperus* (magenta), *Betula* (brown) and *Pinus* (dark green; Kämpf et al., 2022); B. Chironomid-inferred July air temperatures from Bergsee with the reconstructions based on the Swiss-Norwegian calibration dataset excluding *Corynocera ambigua* (red) and based on the Finnish calibration dataset (blue); C. Rarefaction (diversity estimates) of the chironomid assemblages at Bergsee; D. Temperature of Months Above Freezing (TMAF) estimated based on brGDGTs from a site in the Eifel volcanic field, western Germany (Zander et al., 2024); E. $\delta^{18}O$ record from a speleothem of the Sieben Hengste cave system (Luetscher et al., 2015) smoothed with a 11 sample running average; F. Reconstructed glacier advances for the Rhine glacier in the northern Alpine forelands (Preusser et al., 2011); G. $\delta^{18}O$ record of the NGRIP ice core (Rasmussen et al., 2014) smoothed with a 11 sample running average; H. June (orange) and December (blue) insolation at 60°N (Berger and Loutre, 1991). Shaded blue and red zones indicate important climatic events with YD and BA indicating the approximate age of the Younger Dryas and Bølling/Allerød interstadial in records from Bergsee and the Eifel volcanic field, LGM the approximate age of the Last Glacial Maximum in the northern Alpine forelands (Luetscher et al., 2015), GI-2 the age of Greenland interstadials 2 in the NGRIP record (Rasmussen et al., 2014).

elevated nutrient concentrations in the lake (Sæther, 1979; Brodin, 1986) but in small lakes these chironomid taxa are also potentially favoured by a high availability of organic matter. *Daphnia* were the dominant aquatic invertebrate group together with chironomids until 35.6 cal ka BP, but their abundance fluctuated considerably. This could indicate that during certain periods the conditions were favorable for high abundances of *Daphnia* or high production rates of *Daphnia* ephippia. This could be explained by cooler temperatures, presence of predators, changes in the food availability or competition with other invertebrates (Cooper and Smith, 1982; Reede, 1995; Alekseev and Lampert, 2001). The presence of Sialidae mandibles during this zone suggests relatively high limnic production and high organic detritus concentrations in the sediment (Lemdahl, 2000).

Between 30.1 and 23.3 cal ka BP (BER-2) the diversity of the chironomid assemblages decreased drastically suggesting colder conditions (Engels et al., 2020). This period corresponds with the expansion of glaciers to their maximum extent in the northern pre-Alpine region (Ivy-Ochs et al., 2008; Preusser et al., 2011). The presence of the cold stenotherm *Sergentia coracina*-type at high abundances also supports colder temperatures during this zone. In temperate climate conditions, this taxon is usually restricted to the profundal zone of deep, stratified lakes (Brundin, 1949; Sæther, 1979) but it can also thrive in the littoral of lakes under cold climatic conditions (Hofmann, 2001) that probably characterised Bergsee during this period. The high abundances of *Sergentia coracina*-type suggest that profundal taxa were able to colonise shallower zones of the lake, as profundal taxa did not reach these abundances in other parts of the record. Distinct fluctuations between the dominance of *Sergentia coracina*-type and *Parakiefferiella bathophila*-type, a taxon that seems to be representative of warmer climatic conditions, suggest a highly variable climate, at least at the local scale, or a very dynamic lake system. Since it is likely that during the coldest phases *Sergentia coracina*-type colonised the shallower parts of the lake, the expansion of *Parakiefferiella bathophila*-type in the littoral zone relative to *Sergentia coracina*-type during slightly warmer phases would be a possible explanation for the changing abundances of the two taxa. These assemblage shifts may have also been associated with variations in productivity and organic matter availability in the lake, as *Sergentia coracina*-type is common in relatively nutrient-poor lakes (Brundin, 1949; Sæther, 1979) whereas *Parakiefferiella bathophila*-type can also be found in lakes with more nutrients (Moller Pillot, 2013), although both taxa have a wide distribution in respect to nutrients. The presence of *Tanytarsus lugens*-type until 25.6 cal ka BP suggests nutrient-poor conditions in the lake (Sæther, 1979), whereas the presence of *Chaoborus* between 27.1 and 24.3 cal ka BP would agree with seasonally reduced oxygen concentrations in the deep water (Quinlan and Smol, 2010; Ursenbacher et al., 2020). Since *Chaoborus* remains in this interval were only thoracic horns, it was not possible to determine to which morphotype they belonged as they were damaged.

In the following zone (BER-3; 23.3–20.6 cal ka BP), the cold stenotherm *Sergentia coracina*-type disappeared and was replaced by chironomids indicative of warmer conditions such as *Tanytarsus pallidicornis*-type (Heiri et al., 2011). *Parakiefferiella bathophila*-type stayed dominant and sharply increased at the beginning of the zone (22.9 cal ka BP). A similarly abrupt increase in *Parakiefferiella bathophila*-type has been reported from Gerzensee, a small lake on the Swiss Plateau (Brooks, 2000). In this record, the observed increase after the Younger Dryas cold interval was interpreted as a response of the chironomid assemblage to rapid warming of the climate (Brooks, 2000). The taxon was very abundant between 22.9 and 22.2 cal ka BP, reaching a relative abundance of 77 %. Such high percentages of *Parakiefferiella bathophila*-type are not, to our knowledge, reported in any existing European modern calibration datasets, and therefore are presently without any modern or subfossil analogues. *Parakiefferiella bathophila*-type may have reached such high relative abundances because it was already present in the lake in a phase when the diversity of the chironomid fauna was low and may have outcompeted new colonisers arriving when the climate became warmer. Since the taxon can also colonise the deepest part of the lake (Moller Pillot, 2013) it may also have benefited from the disappearance of *Sergentia coracina*-type, presumably due to warmer climate conditions. The increase in the diversity of the chironomid assemblages also agrees with warming climate, as chironomid diversity has been shown to correlate on large spatial and temporal scales with temperature (Engels et al., 2020). *Tanytarsus mendax*-type as well as *Chironomus anthracinus*-type appeared which could potentially indicate an increase of organic matter availability in the sediment (Sæther, 1979; Brodin, 1986).

In the following zone (BER-4; 20.6–16.9 cal ka BP), *Parakiefferiella bathophila*-type decreased drastically suggesting major changes in the lake, since this taxon was present and dominant since the beginning of our record. A similar drop in *Parakiefferiella bathophila*-type abundances have been described for Gerzensee at the beginning of the Younger Dryas (Brooks, 2000). However, in Bergsee the temperature does not seem to have decreased at that time as shown by the abundance of other chironomid taxa that are not necessarily found in cool climate conditions (e.g., *Tanytarsus pallidicornis*-type, *Paratanytarsus penicillatus*-type) and the different climate reconstructions (Fig. 3). Possibly the pronounced decrease in the relative abundances of this taxon is therefore related to other changes in the lake (e.g., organic matter, oxygen). *Tanytarsus pallidicornis*-type and *Paratanytarsus penicillatus*-type are typical of the littoral zone of lakes with the latter often found amongst aquatic plants feeding on periphytic algae (Lods-Crozet and Lachavanne, 1994; Ćerba et al., 2010; Tarkowska-Kukuryk, 2014). Possible changes in habitats and food sources allowed these taxa to outcompete *Parakiefferiella bathophila*-type in Bergsee. *Tanytarsus mendax*-type was replaced by *Chironomus anthracinus*-type in this section, a taxon which is typically found in slightly more nutrient-rich lakes (Sæther, 1979), possibly indicating another rise of organic matter or change of oxygen availability in Bergsee.

In the next zone (BER-5; 16.9–10.7 cal ka BP) the chironomid assemblages changed drastically. *Corynocera ambigua* appeared for the first time in the record and became dominant in two subzones. Between 16.7–14.2 and 12.4–11.2 cal ka BP the taxon reached abundances as high as 75 % of the chironomid assemblages. At present, when this taxon colonises a lake, it is often found in high abundances (Brodersen and Lindegaard, 1999). It has been hypothesised that this could be because the adults cannot fly and therefore stay at the surface of lakes to reproduce which increases their chances to mate compared to other chironomid species (Brodersen and Lindegaard, 1999). *Corynocera ambigua* was originally considered a cold indicator in early studies (Reiss and Gerstmeier, 1984) but it is now well documented that it also occurs in relatively warm lakes in Northern and Eastern Europe (Ashe et al., 2000; Brodersen and Lindegaard, 1999). Brodersen and Lindegaard (1999) attributed high abundances of *Corynocera ambigua* to high oxygen concentration, low nutrient concentration and extensive charophyte beds. The increase of *Plumatella* and Oribatida observed at Bergsee could indicate the development of a macrophyte belt along the shore, as *Plumatella* can profit from these types of habitats (Solhøy, 2001; Wood and Okamura, 2005). The massive and abrupt occurrence of *Corynocera ambigua* in the Bergsee record does not coincide with significant increases in any other cold-indicating chironomid taxa, nor with a decrease in the diversity of the chironomid assemblages, as was observed in earlier phases of cold climatic conditions at Bergsee (BER-2). Therefore, we conclude that the massive increase of *Corynocera ambigua* at Bergsee was not, or only partly or indirectly triggered by changes in temperature conditions. However, it may agree with relatively cool (compare to present) but not necessarily very cold climate conditions, which has major implications for our choice of calibration dataset when reconstructing mean July air temperatures based on the chironomid assemblages (see section 4.2 below). Extremely cold climate conditions ca. 16.9–14.1 cal ka BP at Bergsee, distinctly colder than the preceding period ca. 19–16.9 cal ka BP, would also disagree with palaeoclimate and palaeoenvironmental records from the adjacent Swiss Plateau. No

major decreases in July air temperatures are recorded for this interval in the region (e.g., Bolland et al., 2020) and palaeobotanical evidence indicates the expansion of trees into the shrub tundra characterising this interval (Rey et al., 2017, 2020). The Bølling period is characterised by a distinct decrease in *Corynocera ambigua* at Bergsee. The beginning of this period is marked by a major *Juniperus* peak in the northern Alpine forelands (Ammann et al., 2013; Rey et al., 2017). At Bergsee the start of this phase is dated slightly younger than in other, well-dated palaeoenvironmental records in the region (ca. 14.1 rather than ca. 14.7–14.6 ka BP; Ammann et al., 2013; Rey et al., 2020) due to dating uncertainties in the record and low sample resolution. Taxa presently found in warm lowland lakes in Switzerland, such as *Tanytarsus glabrescens*-type and *Tanytarsus pallidicornis*-type, increased during the phase when *Corynocera ambigua* has low abundances, agreeing with an increase in temperature at the beginning of the Bølling period, which has been recorded by various palaeoclimate archives in the region (Heiri and Lotter, 2005; Lotter et al., 2012; Bolland et al., 2020). A second increase in abundances of *Corynocera ambigua* is centered on the Younger Dryas cold period (12.4–11.2 cal ka BP). In this interval, warm-indicating taxa that expanded at Bergsee during the Bølling and Allerød are again reduced, in agreement with colder conditions. However, the assemblages do not suggest a reversal to extremely cold, arctic environments, as indicated by the persistence of some chironomid taxa common in temperate lowland lakes, such as *Pagastiella*, *Paratanytarsus penicillatus*-type or *Pseudochironomus* and the observation that chironomid diversity does not decrease to the minimum values observed for BER-2. As for the Bølling, the timing of the Younger Dryas slightly differs from other more highly resolved records in the region (e.g., Rey et al., 2020) which place the Younger Dryas from ca. 12.9–11.6 cal ka BP. This can be explained by dating uncertainties in the Bergsee record, but also by the low number of samples in this interval (ca. one sample every 1000 years) not allowing to resolve the very dynamic temperature development during the Lateglacial period and Early Holocene.

Corynocera ambigua disappeared in the last zone (BER-6; 10.7–8.4 cal ka BP) and was replaced by taxa typically found in warm lowland lakes in Switzerland such as *Tanytarsus mendax*-type, *Tanytarsus pallidicornis*-type, *Pseudochironomus*, *Polypedilum nubeculosum*-type *Microtendipes pedellus*-type and *Glyptotendipes pallens*-type (Heiri et al., 2011). This zone corresponds to the onset of the Holocene and warmer climatic conditions are reported for this period (e.g., Heiri et al., 2015). The increasing diversity of the chironomid assemblages also supports warmer conditions (Engels et al., 2020). In this section, chironomids were less dominant in the overall aquatic invertebrate assemblages whereas Ephemeroptera and *Chaoborus* remains became more common. The increase in *Chaoborus*, here *Chaoborus flavicans*-type based on identified mandibles, could suggest a decrease in oxygen concentration in the deepwater (Quinlan and Smol, 2001b; Ursenbacher et al., 2020) and/or an increase in the water temperature as in small lakes *Chaoborus* is usually more abundant in warmer climates (Walker et al., 1997). For example, an increase in *Chaoborus* remains at the beginning of the Holocene has also been documented in Rotsee, a small lake in the northern Swiss lowlands (Stötter, 2015) or in Lac de Champex, a mountain lake in the western Swiss Alps (Perret-Gentil et al., 2023). Typically, Ephemeroptera occur in running water and in the littoral zones of lakes (Brittain, 1974; Brooks et al., 2007; Courtney-Mustaphi et al., 2024). *Plumatella* and Oribatida are still present suggesting a well-structured near-shore area with macrophytes and possibly woody debris (Wood and Okamura, 2005; de la Riva-Caballero et al., 2010; Solhøy, 2001).

The sediment core retrieved from Bergsee is 28.26 m long and considering the depth of the lake before the damming in the 19th century (6 m), Bergsee may have been as deep as ca. 35 m around 45 cal ka BP and 20 m deep ca. 8 cal ka BP. Small lakes in this depth range are often stratified during the summer months, which is supported by the occurrences of *Chaoborus flavicans*-type in different parts of the record. It is unlikely that the decrease in lake depth fundamentally changed the mixing behaviour and the extent of the littoral zones in the lake. Nevertheless, the long-term decrease in water depth may have influenced the limnology (e.g., oxygen, organic matter, light, habitat availability) and the invertebrate assemblages. However, the most pronounced changes in the invertebrate assemblage composition over the 39 kyr-long record seem to mainly represent abrupt centennial to millennial-scale changes rather than long-term multimillennial-scale trends. This suggests that climatic variations and centennial to millennial-scale changes in in-lake conditions may have been more relevant for the invertebrate assemblages than the regular long-term decrease in water depth due to the infilling of the lake.

4.2. Comparison of temperature reconstructions based on different calibration datasets

Three different temperature reconstructions with two calibration datasets (Swiss-Norwegian and Finnish) have been calculated in the present study. Initial reconstructions were calculated with a calibration dataset and WA-PLS inference model based on lakes from northern, central and southern Norway and the northern Swiss lowlands and the Swiss Alps (Heiri et al., 2011). The dataset contains a wide range of lake types and bedrock conditions, although the Swiss sites, particularly the lowland sites, are mainly on carbonate or mixed bedrock, whereas Bergsee is located on granite and gneiss bedrock characteristic of the Black Forest region (Becker et al., 2004). This model and calibration dataset have been widely used in Central Europe to reconstruct temperatures from chironomid records (e.g., Millet et al., 2012; Samartin et al., 2012; Tóth et al., 2012; Bolland et al., 2020). However, when applied to the Bergsee record this temperature inference model indicated very unusual and unlikely temperatures for part of the record. Whereas temperatures seemed realistic for BER1–4 and 6 (see discussions in sections 4.3 below), they appear too low in sections of BER-5 dominated by *Corynocera ambigua* compared to other available palaeoclimate data for the region. For example, temperatures of ca. 8.7 °C are reconstructed with this model for the period preceding the Bølling (16.1–14.8 cal ka BP) and ca. 9.4 °C for the period representing the Younger Dryas (12.4 cal ka BP). For the same period, temperatures in the range of 10.8–12.4 °C (before the Bølling; Heiri and Millet, 2005; Larocque-Tobler et al., 2010; Lotter et al., 2012) and 13.3–15.9 °C (Younger Dryas; Heiri and Millet, 2005; Larocque-Tobler et al., 2010) are recorded from localities in Switzerland and France if they are adjusted to the elevation of Bergsee based on modern temperature laps rates of 0.6 °C per 100 m of altitude (Livingstone et al., 1999). Summer air temperatures as low as 8.8 °C have been reconstructed at Burgäschisee, Swiss Plateau, before the Bølling (Bolland et al., 2020). However, these low temperatures are inferred for the period preceding 16 cal ka BP at Burgäschisee, and not the interval 16.1–14.8 cal ka BP as at Bergsee. The taxon in the Bergsee record responsible for these unusually low reconstructed temperatures, *Corynocera ambigua*, is presently largely absent in small lakes in the southern sector of Central Europe and therefore not represented in the Swiss lakes of the Swiss-Norwegian calibration dataset, but only in Norwegian lakes with maximum abundances in lakes with July air temperatures of 8–12 °C (Heiri et al., 2011). The temperature optimum of this taxon in the Swiss-Norwegian calibration dataset is 10 °C with a tolerance of 1 °C (Heiri et al., 2011). However, in other calibration datasets the optimum of *Corynocera ambigua* is considerably higher and the distribution broader. For example, in the Finnish calibration dataset of Luoto et al. (2014) the optimum is 12.4 °C and tolerance 1.8 °C or in the Russian calibration dataset of Nazarova et al. (2015) the optimum is 12.9 °C but with an even broader temperature tolerance range of 3.6 °C. Since it was obvious that the optimum of *Corynocera ambigua* had a strong impact on reconstructed temperatures during BER-5, and the optimum of the taxon in the Swiss-Norwegian calibration dataset was not representative of the full distribution of *Corynocera ambigua* relative to summer temperature, we also calculated a second reconstruction based on the Swiss-Norwegian calibration dataset excluding this taxon. Some previous studies have also calculated

temperature reconstructions without this taxon although it was not specifically excluded. For example, Heiri and Millet (2005) and Larocque-Tobler et al. (2010) used the Swiss calibration dataset to reconstruct temperatures from their records, at Lac Lautrey and Egelsee respectively, which included *Corynocera ambigua*. However, since this taxon is not present in the modern calibration dataset from Switzerland, it did not influence the reconstructed temperatures. However, with some few exceptions (e.g., von Gunten et al., 2008), selective deletion of individual species or taxa has only rarely been attempted in chironomid-based temperature reconstruction and the effects of such deletions have not been systematically explored. To assess whether the overall pattern of reconstructed temperatures inferred based on the Swiss-Norwegian calibration dataset excluding *Corynocera ambigua* could be reproduced by another, independent calibration dataset and inference model, we also calculated a third reconstruction based on a calibration dataset from Finland (Luoto et al., 2014). This dataset covers a smaller temperature gradient than the Swiss-Norwegian dataset, is based on a lower number of sampled sites and, since it includes only lakes from Fennoscandia, it covers less diverse lake types than the Swiss-Norwegian dataset. However, *Corynocera ambigua* covers a wider, and presumably more realistic temperature range in this dataset.

Overall, the July air temperature estimates with the two models based on the Swiss-Norwegian calibration dataset are similar with the exception of the period which contains high relative abundances of *Corynocera ambigua* (Fig. 3). Considering the problem related to this taxon mentioned above, we believe the reconstruction calculated with the Swiss-Norwegian calibration dataset excluding *Corynocera ambigua* is probably more realistic when this taxon is abundant. The temperature estimates calculated with the Finnish calibration dataset show a similar temperature development to the one calculated with the Swiss-Norwegian calibration dataset excluding *Corynocera ambigua*, with the coldest interval ca. 30.1–23.3 cal ka BP when the diversity of the chironomid assemblages is the lowest and other palaeorecords suggest an extension of glaciers to their maximum extent in the northern Alpine foreland and cool temperatures (see section 4.3 below). However, reconstructions based on the Finnish calibration dataset suggest a more pronounced warming after this period (i.e., a phase of warmer temperatures ca. 23.2–19.5 cal ka BP) and overall slightly lower temperatures in the Lateglacial sections of the record including the Bølling/Allerød interstadial and the Younger Dryas cold period (Fig. 4). Relative changes in the two reconstructions are, however, very similar in the phase when *Corynocera ambigua* is present at Bergsee. This confirms that the main temperature changes apparent in the reconstruction based on the Swiss-Norwegian calibration dataset excluding *Corynocera ambigua* can be reproduced by a model relying on another calibration dataset where this taxon is included but present over a broader temperature gradient than in the Swiss-Norwegian dataset.

Looking at the modern analogue and goodness-of-fit statistics, the Swiss-Norwegian calibration dataset seems to be more suitable for the Bergsee record than the Finnish dataset for which only two fossil samples from Bergsee have good analogues (Fig. 3). This could be because the Finnish calibration dataset includes less lakes than the Swiss-Norwegian dataset (Velle et al., 2010). For the reconstruction based on the Swiss-Norwegian calibration dataset, good analogues are available for most of the record, with the exception of samples covering the Bølling/Allerød interstadial, Younger Dryas and Early Holocene. Goodness-of-fit statistics indicate that the assemblages in the coldest part of the record (ca. 30.1–23.3 cal ka BP) are most unusual when compared to the calibration datasets. This is not surprising considering the low diversity of these samples and the unusual combination of high abundances of *Parakiefferiella bathophila*-type and *Sergentia coracina*-type in this part of the record. However, WA-PLS performs relatively well in non-analogues situations, and with unusual assemblages, as long as the dominant species are well represented in the calibration dataset (ter Braak, 1995; Birks et al., 2010). The poorer analogue and goodness-of-fit situation for the Finnish dataset and individual samples for the Swiss-Norwegian dataset therefore does not necessarily mean that the reconstructed temperature values are not reliable (e.g., Heiri et al., 2003; Heiri et al., 2007). However, considering the less favorable analogue statistics, the temperature estimates calculated with the Finnish model have to be interpreted with caution even though they appear realistic when compared to previous reconstructions (e.g., Heiri and Millet, 2005; Larocque-Tobler et al., 2010; Lotter et al., 2012; Bolland et al., 2020).

The temperature gradient of the Swiss-Norwegian calibration dataset is considerably larger than the Finnish dataset which provides a major advantage especially when reconstructing temperature at the cold end of the gradient (Brooks and Birks, 2001). The RMSEP of the Finnish inference model (0.88 °C) is smaller than that of the Swiss-Norwegian model, both with and without *Corynocera ambigua* (1.40 and 1.43 °C respectively). This is most likely because of the shorter temperature gradient included in the Finnish calibration dataset. Also, the Swiss-Norwegian calibration dataset includes many mountain lakes located in catchments with complicated topography. In such situations, estimated July air temperature, used for calculating the prediction errors, may not be as representative for actual air and water temperatures as in the Finnish dataset which includes many lowland lakes at different latitudes. In contrast, fewer taxa are represented in the Finnish calibration dataset. As a consequence, some rare taxa found in Bergsee were not used to calculate the corresponding temperature reconstruction (e.g., *Diamesa aberrata*-type, *Heleniella*, *Parachironomus varus*-type). The Swiss-Norwegian and the Finnish calibration datasets include lakes with up to 18 and 17 °C mean July air temperature, respectively (Heiri et al., 2011; Luoto et al., 2014). At the same time Bergsee is a lowland lake at lower elevation than similar lakes on the Swiss Plateau with estimated mean July air temperature presently around 20.3 °C (see section 2.1). Earlier quantitative temperature reconstructions in the region have suggested similar temperatures during the Bølling/Allerød period and Early Holocene as recorded in the late Holocene (e.g., Heiri et al., 2014). This suggests that chironomid-inferred estimates in the Bergsee record, particularly during the Early Holocene interval, may already have been affected by the edge effect, since temperatures may have reached values close to or exceeding the warmer limit of temperature in the calibration datasets. In addition, the strong increase in *Chaoborus* suggests that Bergsee may have become seasonally anoxic in this interval. This may also potentially have influenced chironomid-inferred temperature values, as hypoxia may have similarly strong, or stronger, influence on bottom-water chironomid assemblages in small, stratified lakes than temperatures during the summer months (e.g., Quinlan and Smol, 2001b; Heiri et al., 2003; Perret-Gentil et al., 2023). Based on the geographical location of Bergsee and the arguments outlined above, we consider, the Swiss-Norwegian calibration dataset with *Corynocera ambigua* excluded to probably be the most suitable calibration dataset for the Bergsee record. However, the observation that the temperature reconstructions calculated with the Swiss-Norwegian calibration dataset excluding *Corynocera ambigua* and the Finnish dataset seem to follow the same trends, with a considerable overlap of the reconstructions considering the estimated prediction errors, suggests that both reconstructions provide realistic past summer temperature trends. In contrast, sections of the reconstruction with high abundances of *Corynocera ambigua* should be interpreted with caution, due to the uncertain thermal ecology of this taxon, and the highest reconstructed values during the Bølling/Allerød and the Early Holocene may have been affected by the edge effect and hypoxic conditions in Bergsee during these intervals.

4.3. Comparison with other studies

As discussed in detail in section 4.2 above, mean July air temperature reconstructions calculated based on the Swiss-Norwegian calibration dataset excluding *Corynocera ambigua* and the Finnish dataset, the two reconstructions we consider the most realistic, show very similar

trends. Low values are inferred for most of the examined interval before ca. 15–14 cal ka BP and minimum temperatures are reconstructed around 30.1–23.3 cal ka BP. The reconstructed temperature rises during the Bølling/Allerød interstadial and Early Holocene, with a clear and pronounced cooling registered in the intercalated Younger Dryas cold period, although the reconstruction does not have a high enough sampling resolution in this part of the sequence to record these variations in detail (Fig. 4).

In the first zone (45.4–30.1 cal ka BP), the temperature estimates are overall relatively stable (mean: 11.7 °C) except for two short periods with abrupt increase in temperature to 13.1 and 13.2 °C around 38.5 and 32.7 cal ka BP respectively. Another chironomid-inferred temperature reconstruction was developed for Unterangerberg, located at 630 m a.s.l. in the Austrian northern Alps, between ca. 55–41 cal ka BP (Ilyashuk et al., 2022). The reconstructed mean July air temperature estimates at Unterangerberg are comparable to our study, for the same time period, ranging from 10 to 13 °C (Fig. 4), even though the site is located at slightly higher altitudes than Bergsee (Ilyashuk et al., 2022). However, in the Unterangerberg study the authors have included *Corynocera ambigua* to calculate their temperature reconstruction making the comparison with our reconstruction excluding this taxon difficult. Based on pollen analyses of the Bergsee sediments, eight phases of forest development were described in this interval, with increases of *Pinus* and *Betula* pollen respectively, potentially corresponding to Dansgaard-Oeschger events with warmer temperature and more humid conditions (Duprat-Oualid et al., 2017). However, chironomid-inferred temperatures only indicate a temperature increase during one of these (ca. 32.7 cal ka BP; Fig. 4). This discrepancy between the pollen record and chironomid-inferred temperatures could partly be explained by the lower resolution of the chironomid record. However, a more detailed comparison shows that around 45.4 and 38.5 cal ka BP relatively warm chironomid-inferred temperature estimates occurred during transitions to more steppe and tundra-like pollen assemblages (Fig. 4; Duprat-Oualid et al., 2017). This would suggest that these shifts towards more open vegetation were not primarily caused by cooling, as would be expected if summer temperatures were driving these changes, but rather variations in humidity or temperatures during seasons other than summer (Lotter et al., 2012). Nevertheless, the reconstructed mean July air temperature around 11–12 °C indicates that during this interval climatic conditions during the summer may have already been close to those characterising treeline environments, as these have typically been considered to be around 7.5–9.5 °C mean July air temperature in dry and continental conditions (Landolt et al., 2015).

BER-2 (30.1–23.3 cal ka BP) corresponds to the coldest period of the record with average July air temperature estimated to 10.5 and 11.3 °C for the reconstructions based on the Swiss-Norwegian calibration set with *Corynocera ambigua* excluded and the Finnish dataset, respectively. This period corresponds to the onset of the LGM worldwide (Clark et al., 2009) which was triggered by low northern summer insolation (Berger and Loutre, 1991; Laskar et al., 2004) and atmospheric CO_2 concentration (Ahn et al., 2004). Based on marine records the maximum extent of ice coverage globally was reached around 27.5–23.3 ka BP (Hughes et al., 2013). At a more regional scale, the Alpine glaciers reached their maximum extent between 26 and 22 cal ka BP in the northern Alpine forelands as reconstructed based on glaciological evidence (e.g., Preusser et al., 2011; Monegato et al., 2017; Kamleitner et al., 2023). This age corresponds to the maximum extent of the Reuss glacier which was reconstructed to have its maximum position around 25–22 ka BP at Birmenstorf ca. 30 km from Bergsee (Kamleitner et al., 2023). This phase of maximum glacier extent apparently occurred during the latter part of the interval 30.1–23.3 cal ka BP with minimum July air temperatures. However, it had to have been preceded by an interval of pronounced glacier growth, which, based on our palaeotemperature data, occurred during a phase of particularly low summer temperatures in the northern Alpine forelands. The timing of the maximum extent of ice cover in the Black Forest is still unknown and could have been delayed due to the leeward position of this mountain range relative to the Alps (Hofmann et al., 2020). Atmospheric circulation seems to have been characterised by the advection of humid air masses coming from the Mediterranean Sea during the Last Glacial Maximum (Luetscher et al., 2015; Monegato et al., 2017), leading to less precipitation and ice build-up in the Black Forest (Hofmann et al., 2020), but local palaeoclimate records are rare during this period for the Black Forest region. The pollen record of Bergsee also suggests cold and dry climate at that time as shown by the high abundances of dry grassland vegetation and very low abundance or absence of boreal pollen types (Duprat-Oualid et al., 2017). Two periods seem to have been particularly dry and cold based on the pollen: 30.3–28.3 and 24.8–23.2 cal ka BP (ages updated with the chronology used in the present paper; Duprat-Oualid et al., 2017). The first episode corresponds to a strong decrease of reconstructed mean July air temperature and the second matches with the lowest diversity values and highest abundances of the cold stenotherm *Sergentia coracina*-type in the Bergsee record (Fig. 4). Oxygen isotopes analysed in the speleothem record from the Sieben Hengste cave system, located in the northern Alps, also indicate a distinct minimum in $\delta^{18}O$ during this time (Luetscher et al., 2015), although variations in this record have been interpreted to predominantly reflect changes in moisture source, with minimum values reflecting a southward shift in storm tracks during the Alpine LGM. Estimated mean July air temperatures calculated with the different calibration datasets for this phase decrease to ca. 9.4 °C with the Swiss-Norwegian model with *Corynocera ambigua* excluded and 10.6 °C with the Finnish model. These temperature estimates are ca. 10 °C colder than the present mean July air temperature at Bergsee estimated to ca. 20.3 °C (see section 2.1). Mean temperatures for the months above freezing (TMAF) were reconstructed based on a branched glycerol dialkyl glycerol tetraether (brGDGT) record from the Eifel volcanic field, western Germany (Zander et al., 2024). In this record, minimum temperatures were also reconstructed for the same period as in Bergsee, supporting our reconstruction based on fossil chironomids (Fig. 4). The period of the LGM is a widely used target for climate modelling experiments to assess temperatures but also intercomparability of climate models during a recent phase of minimum temperatures in the late Quaternary. However, these simulations often use a slightly younger age of 21 cal ka BP as target. Available climate model simulations seem to converge on mean July air temperature values around 8–12 °C in Central Europe during the LGM (e.g., Kim et al., 2003; Strandberg et al., 2011; Russo et al., 2024). For 21 cal ka BP, the mean July air temperature estimates calculated from the chironomid assemblages of Bergsee indicate slightly warmer temperatures with 12.8 and 13.5 °C respectively for the reconstructions based on the Swiss-Norwegian calibration dataset with *Corynocera ambigua* excluded and the Finnish calibration dataset. However, the values from climate model simulations agree very well with the temperature inferred from the chironomids at Bergsee during the regional LGM ca. 26.5–23.5 cal ka BP.

After the minimum temperatures coinciding with the LGM in the northern Alpine forelands, a sharp increase of about 2.3 °C in mean July air temperature is estimated at Bergsee based on the Swiss-Norwegian model excluding *Corynocera ambigua*, with an even more pronounced increase (2.8 °C) reconstructed based on the Finnish calibration dataset. This temperature increase is supported by an increase in the diversity of the chironomid assemblages (Fig. 4; Engels et al., 2020). Glaciers in the northern Alpine forelands started to retreat as early as 22 cal ka BP for the Reuss glacier and probably around 23 cal ka BP for the Rhine glacier (Kamleitner et al., 2023). A strong increase of ca. 4 °C in TMAF was also recorded from the Eifel volcanic field in western Germany at that time (Zander et al., 2024). This increase in temperature may be linked to Greenland interstadial 2.2 (Rasmussen et al., 2014). Subsequent readvances of glacier fronts occurred in the northern Alpine region as well as in the Black Forest (Hofmann et al., 2022; Kamleitner et al., 2023). Possibly a phase of cooler temperature indicated by both reconstructions at Bergsee around 19.2 cal ka BP may have been related to and may have

favoured one of these glacier advances.

Several chironomid-inferred temperature reconstructions are already available for the Lateglacial Period and Early Holocene (BER-5; 16.9–10.7 cal ka BP) for the northern Alpine forelands and the Jura mountains. For example, at Burgäschisee, situated at 465 m a.s.l. on the Swiss Plateau, mean July air temperatures were estimated at 9 °C around 17 cal ka BP and rose to 15 °C at 13 cal ka BP during the Bølling/Allerød interstadial (Bolland et al., 2020). At Lac Lautrey, a small lake at 788 m a.s.l. in the French Jura mountains, July air temperature increased from 10 °C around 15 cal ka BP to 16 °C around 13 cal ka BP (Heiri and Millet, 2005). At Gerzensee, situated at 603 m a.s.l. in the foothills of the northern Bernese Alps, Switzerland, inferred July air temperature ranged from 10.5 to 16 °C between 15.5 and 13 cal ka BP (Lotter et al., 2012). The absolute inferred temperature values differ to some extent between the reconstructions, partly due to altitudinal differences between sites and presumably different topographies and local climates as well as the use of different calibration datasets. However, they show a very comparable increase in inferred temperatures in this interval as at Bergsee, where reconstructed temperatures increased from ca. 12.1 to 16.5 °C between 16.1 and 13.6 cal ka BP based on the Swiss-Norwegian calibration dataset excluding *Corynocera ambigua* and from ca. 11.1 to 15.5 °C based on the Finnish calibration dataset. Temperature reconstructions in the Alpine region consistently indicate a rapid temperature increase at the beginning of the Bølling (ca. 14.7–14.6 cal ka BP) and a distinct cooling during the Younger Dryas (Heiri et al., 2014). Unfortunately, these sections of the Bergsee chironomid record are not analysed at high enough resolution to resolve these climate variations in detail. However, the temperature reconstructions based on the Swiss-Norwegian calibration dataset with *Corynocera ambigua* excluded and the Finnish calibration dataset clearly show major variations in temperature during these climate events. The increase in temperatures during the Bølling/Allerød is estimated to ca. 4 °C based on the two models respectively, which agrees well with estimated increases in the region (Heiri and Millet, 2005; Lotter et al., 2012; Bolland et al., 2020). During the Younger Dryas, reconstructed temperatures based on both models decrease by ca. 3–4 °C respectively, which is in the upper range of temperature decreases recorded from other sites in the region which generally range from ca. 1.5–4.5 °C (Heiri and Millet, 2005; Larocque-Tobler et al., 2010; Samartin et al., 2012; Heiri et al., 2015). As discussed earlier the amplitude of these changes are clearly more realistic and comparable with other regional palaeotemperature records in the reconstruction based on the Swiss-Norwegian calibration dataset with *Corynocera ambigua* excluded and the Finnish calibration dataset than in the reconstruction based on the Swiss-Norwegian calibration dataset with *Corynocera ambigua* included. In the latter reconstruction the temperature variations have been estimated to ca. 6–7 °C, clearly exceeding reconstructed changes at other sites. Nevertheless, the comparatively large mean July air temperature changes inferred in the Bergsee chironomid record for the Younger Dryas, even excluding *Corynocera ambigua* from the Swiss-Norwegian calibration dataset, suggests that cooling during this event may have been particularly pronounced in the vicinity of Bergsee or reinforced by other environmental conditions (e.g., local hydrology or other limnological changes) during this interval.

5. Conclusion

We provide the first quantitative, chironomid-based July air temperature reconstructions for the period covering the LGM from the southwestern part of Central Europe. Our reconstructions indicate that the coldest period, with inferred mean July air temperature in the range of 10.5 °C, occurred between 30.1 and 23.3 cal ka BP at Bergsee, which is about 10 °C colder than the present mean July air temperature. This period corresponds to the maximum glacier advances in the northern Alpine forelands and also coincides with the preferential advection of moisture from the south across the Alps (Luetscher et al., 2015), and minimum temperatures occurring at the time of Heinrich event 2 as reconstructed based on brGDGTs for a record from western Germany (Zander et al., 2024). The temperatures reconstructed based on the Swiss-Norwegian calibration dataset excluding *Corynocera ambigua* and the Finnish calibration dataset, the reconstructions we consider most reliable, show an increase after this interval by 2.3 and 2.8 °C respectively and stayed in the range of 12.5 °C in the period ca. 23–15 cal ka BP. Then a major increase in temperatures by ca. 4 °C is reconstructed at the beginning of the Bølling followed by a cooling of ca. 4 °C during the Younger Dryas which are both well represented in our record. In contrast and as discussed in detail above, reconstructions based on the Swiss-Norwegian calibration dataset with *Corynocera ambigua* included provide unexpectedly low temperatures for the periods 16.7–14.7 and 12.4–11.2 cal ka BP which do not agree with other regional temperature reconstructions. We show that these low reconstructed temperatures can be attributed to the limited distribution of *Corynocera ambigua* in the Swiss-Norwegian calibration dataset, which does not cover the full range of summer temperature conditions in which this taxon can occur at, and therefore we consider this reconstruction less reliable than the two reconstructions mentioned before.

Our new quantitative mean July air temperature reconstruction from Bergsee helps to fill a major gap of knowledge on climatic conditions during the maximum extent of the Würmian glaciation in southwestern parts of Central Europe. This will hopefully contribute to a better understanding of climate development during the Last Glacial Period. The Bergsee record, together with earlier chironomid-based reconstructions from the region developed for Füramoos, southern Germany (Bolland et al., 2021) and Unterangerberg, Austria (Ilyashuk et al., 2022) provide chironomid-based temperature estimates across most of the Würmian glaciation. As a consequence, chironomid-inferred palaeotemperature estimates can now complement other quantitative palaeotemperature proxies such as pollen (e.g., Guiot et al., 1993), brGDGTs (e.g., Zander et al., 2024), oxygen isotopes in speleothem records (e.g., Luetscher et al., 2015) and glacier dynamics (e.g., Heiri et al., 2014) for understanding both relative temperature changes between the LGM and other key late Quaternary climate periods and absolute temperatures during this crucial phase of the late Quaternary period in Europe.

CRediT authorship contribution statement

Pierre Lapellegerie: Formal analysis, Investigation, Data curation, Writing – original draft, Writing – review & editing, Visualization. **Laurent Millet:** Conceptualization, Writing – review & editing. **Damien Rius:** Writing – review & editing. **Fanny Duprat-Oualid:** Investigation, Writing – review & editing. **Tomi Luoto:** Writing – review & editing. **Oliver Heiri:** Conceptualization, Investigation, Writing – original draft, Writing – review & editing, Visualization, Funding acquisition.

Declaration of competing interest

The authors declare that they have no known competing financial interests or personal relationships that could have appeared to influence the work reported in this paper.

Acknowledgements

We thank two anonymous reviewers and editor Patrick Rioual for valuable and constructive comments on the manuscript. We would like to thank all members of the field work team: Julien Didier, Simon Belle, Fabien Arnaud and Bernard Fanget. Further thanks go to Sönke Szidat and the Laboratory for the Analysis of Radiocarbon with AMS (LARA) at the University of Bern for additional ^{14}C dating within the Lateglacial Interstadial. We also thank Martin Hofmann for useful information concerning the chronology of the Black Forest glaciers and Sandra Brügger for help with drawing the figures. This research has been supported by the Swiss National Science Foundation (SNF grant

200021_165494).

Appendix A. Supplementary data

Supplementary data to this article can be found online at https://doi.org/10.1016/j.quascirev.2024.109016.

Data availability

The chironomid counts, percentages and temperature reconstructions as well as the calibration datasets are available in the supplementary information

References

Ahn, J., Wahlen, M., Deck, B.L., Brook, E.J., Mayewski, P.A., Taylor, K.C., White, J.W.C., 2004. A record of atmospheric CO_2 during the last 40,000 years from the Siple Dome, Antarctica ice core. J. Geophys. Res. 109, 2003JD004415. https://doi.org/10.1029/2003JD004415.

Alekseev, V., Lampert, W., 2001. Maternal control of resting-egg production in *Daphnia*. Nature 414, 899–901. https://doi.org/10.1038/414899a.

Ammann, B., Van Leeuwen, J.F.N., Van Der Knaap, W.O., Lischke, H., Heiri, O., Tinner, W., 2013. Vegetation responses to rapid warming and to minor climatic fluctuations during the Late-Glacial Interstadial (GI-1) at Gerzensee (Switzerland). Palaeogeogr. Palaeoclimatol. Palaeoecol. 391, 40–59. https://doi.org/10.1016/j.palaeo.2012.07.010.

Ampel, L., Bigler, C., Wohlfarth, B., Risberg, J., Lotter, A.F., Veres, D., 2010. Modest summer temperature variability during DO cycles in western Europe. Quat. Sci. Rev. 29, 1322–1327. https://doi.org/10.1016/j.quascirev.2010.03.002.

Antoine, P., Rousseau, D.-D., Degeai, J.-P., Moine, O., Lagroix, F., Kreutzer, S., Fuchs, M., Hatté, C., Gauthier, C., Svoboda, J., Lisá, L., 2013. High-resolution record of the environmental response to climatic variations during the Last Interglacial–Glacial cycle in Central Europe: the loess-palaeosol sequence of Dolní Věstonice (Czech Republic). Quat. Sci. Rev. 67, 17–38. https://doi.org/10.1016/j.quascirev.2013.01.014.

Armitage, P.D., Cranston, P.S., Pinder, L.C.V., 1995. The Chironomidae: the Biology and Ecology of Non-biting Midges. Springer, Netherlands, Dordrecht. https://doi.org/10.1007/978-94-011-0715-0.

Ashe, P., McCarthy, T.K., Fahy, S., 2000. The supposed arctic relict *Corynocera ambigua* Zetterstedt in Ireland (Diptera: chironomidae), with a review of its ecology and distribution. Verh. internat. Ver. Limnol. 27, 267–272. https://doi.org/10.1080/03680770.1998.11901238.

Becker, A., Angelstein, S., 2004. Rand- und subglaziale Rinnen in den Vorbergen des Süd-Schwarzwaldes bei Bad Säckingen, Hochrhein. E&G Quaternary Sci. J. 54, 1–19. https://doi.org/10.3285/eg.54.1.01.

Becker, A., Bucher, F., Davenport, C.A., Flisch, A., 2004. Geotechnical characteristics of post-glacial organic sediments in Lake Bergsee, southern Black Forest, Germany. Eng. Geol. 74, 91–102. https://doi.org/10.1016/j.enggeo.2004.03.003.

Becker, A., Ammann, B., Anselmetti, F.S., Hirt, A.M., Magny, M., Millet, L., Rachoud, A.-M., Sampietro, G., Wüthrich, C., 2006. Paleoenvironmental studies on lake bergsee, Black forest, Germany. N. Jb. Geol. Paläont. Abh. 240, 405–445. https://doi.org/10.1127/njgpa/240/2006/405.

Bennett, K.D., 1996. Determination of the number of zones in a biostratigraphical sequence. New Phytol. 132, 155–170. https://doi.org/10.1111/j.1469-8137.1996.tb04521.x.

Berger, A., Loutre, M.F., 1991. Insolation values for the climate of the last 10 million years. Quat. Sci. Rev. 10, 297–317. https://doi.org/10.1016/0277-3791(91)90033-Q.

Birks, H.J.B., Line, J.M., Juggins, S., Stevenson, A.C., ter Braak, C.J.F., 1990. Diatoms and pH reconstruction. Phil. Trans. Roy. Soc. Lond. B 327, 263–278. https://doi.org/10.1098/rstb.1990.0062.

Birks, H.J.B., Line, J.M., 1992. The use of rarefaction analysis for estimating palynological richness from quaternary pollen-analytical data. Holocene 2, 1–10. https://doi.org/10.1177/095968369200200101.

Birks, H.J.B., Heiri, O., Seppä, H., Bjune, A.E., 2010. Strengths and weaknesses of quantitative climate reconstructions based on late-quaternary biological proxies. Open J. Ecol. 3, 68–110. https://doi.org/10.2174/1874213001003020068.

Blaauw, M., Christen, J.A., Vazquez, J.E., Goring, S., 2022. clam: classical age-depth modelling of cores from depositis. R package version 2.5.0. https://CRAN.R-project.org/package=clam.

Bolland, A., Rey, F., Gobet, E., Tinner, W., Heiri, O., 2020. Summer temperature development 18,000–14,000 cal. BP recorded by a new chironomid record from Burgäschisee, Swiss Plateau. Quat. Sci. Rev. 243, 106484. https://doi.org/10.1016/j.quascirev.2020.106484.

Bolland, A., Kern, O.A., Allstädt, F.J., Peteet, D., Koutsodendris, A., Pross, J., Heiri, O., 2021. Summer temperatures during the last glaciation (MIS 5c to MIS 3) inferred from a 50,000-year chironomid record from Füramoos, southern Germany. Quat. Sci. Rev. 264, 107008. https://doi.org/10.1016/j.quascirev.2021.107008.

Bolland, A., Kern, O.A., Koutsodendris, A., Pross, J., Heiri, O., 2022. Chironomid-inferred summer temperature development during the late Rissian glacial, Eemian interglacial and earliest Würmian glacial at Füramoos, southern Germany. Boreas 51, 496–516. https://doi.org/10.1111/bor.12567.

Bond, G., Heinrich, H., Broecker, W., Labeyrie, L., McManus, J., Andrews, J., Huon, S., Jantschik, R., Clasen, S., Simet, C., Tedesco, K., Klas, M., Bonani, G., Ivy, S., 1992. Evidence for massive discharges of icebergs into the North Atlantic ocean during the last glacial period. Nature 360, 245–249. https://doi.org/10.1038/360245a0.

Brittain, J.E., 1974. Studies on the lentic Ephemeroptera and Plecoptera of southern Norway. Norsk. Ent. Tidskr. 21, 135–154.

Brodersen, K.P., Lindegaard, C., 1999. Mass occurrence and sporadic distribution of *Corynocera ambigua* Zetterstedt (Diptera, Chironomidae) in Danish lakes. Neo- and palaeolimnological records. J. Paleolimnol. 22, 41–52. https://doi.org/10.1023/A:1008032619776.

Brodersen, K.P., Odgaard, B.V., Vestergaard, O., Anderson, N.J., 2001. Chironomid stratigraphy in the shallow and eutrophic Lake Søbygaard, Denmark: chironomid-macrophyte co-occurrence: chironomid stratigraphy in Lake Søbygaard. Freshw. Biol. 46, 253–267. https://doi.org/10.1046/j.1365-2427.2001.00652.x.

Brodin, Y.W., 1986. The postglacial history of lake flarken, southern Sweden, interpreted from subfossil insect remains. Int. Revue ges. Hydrobiol. Hydrogr. 71, 371–432. https://doi.org/10.1002/iroh.19860710313.

Broecker, W., Bond, G., Klas, M., Clark, E., McManus, J., 1992. Origin of the northern Atlantic's Heinrich events. Clim. Dynam. 6, 265–273. https://doi.org/10.1007/BF00193540.

Brooks, S.J., 2000. Late-glacial fossil midge stratigraphies (insecta: Diptera: chironomidae) from the Swiss Alps. Palaeogeogr. Palaeoclimatol. Palaeoecol. 159, 261–279. https://doi.org/10.1016/S0031-0182(00)00089-4.

Brooks, S.J., Birks, H.J.B., 2001. Chironomid-inferred air temperatures from Lateglacial and Holocene sites in north-west Europe: progress and problems. Quat. Sci. Rev. 20, 1723–1741. https://doi.org/10.1016/S0277-3791(01)00038-5.

Brooks, S.J., Langdon, P.G., Heiri, O., 2007. The identification and use of Palaearctic Chironomidae larvae in palaeoecology. Quaternary Research Association, 276p. London.

Brundin, L., 1949. Chironomiden und andere Bodentiere der südschwedischen Urgebirgsseen: Ein Beitrag zur Kenntnis der bodenfaunistischen Charakterzüge schwedischer oligotropher Seen. In: Carl Blom, Lund (Eds.), Intitut of Freshwater Research, Drottningholm.

Čerba, D., Mihaljević, Z., Vidaković, J., 2010. Colonisation of temporary macrophyte substratum by midges (Chironomidae: Diptera). Ann. Limnol. - Int. J. Lim. 46, 181–190. https://doi.org/10.1051/limn/2010015.

Chaline, J., Jerz, H., 1984. Arbeitsergebnisse der Subkommission für Europäische Quartärstratigraphie Stratotypen des Würm-Glazials. Eiszeitalt. Ggw. 35, 185–206.

Clark, P.U., Dyke, A.S., Shakun, J.D., Carlson, A.E., Clark, J., Wohlfarth, B., Mitrovica, J. X., Hostetler, S.W., McCabe, A.M., 2009. The last glacial maximum. Science 325, 710–714. https://doi.org/10.1126/science.1172873.

Cooper, S.D., Smith, D.W., 1982. Competition, predation and the relative abundances of two species of *Daphnia*. J. Plankton Res. 4 (4), 859–879. https://doi.org/10.1093/plankt/4.4.859.

Courtney-Mustaphi, C.J., Steiner, E., Von Fumetti, S., Heiri, O., 2024. Aquatic invertebrate mandibles and sclerotized remains in Quaternary lake sediments. J. Paleolimnol. 71, 45–83. https://doi.org/10.1007/s10933-023-00302-y.

Dansgaard, W., Johnsen, S.J., Clausen, H.B., Dahl-Jensen, D., Gundestrup, N.S., Hammer, C.U., Hvidberg, C.S., Steffensen, J.P., Sveinbjörnsdottir, A.E., Jouzel, J., Bond, G., 1993. Evidence for general instability of past climate from a 250-kyr ice-core record. Nature 364, 218–220. https://doi.org/10.1038/364218a0.

Dawidowicz, P., Pijanowska, J., Ciechomski, K., 1990. Vertical migration of *Chaoborus* larvae is induced by the presence of fish. Limnol. Oceanogr. 35, 1631–1637. https://doi.org/10.4319/lo.1990.35.7.1631.

de Beaulieu, J.-L., Reille, M., 1992. The last climatic cycle at La Grande Pile (Vosges, France) a new pollen profile. Quat. Sci. Rev. 11, 431–438. https://doi.org/10.1016/0277-3791(92)90025-4.

de la Riva-Caballero, A., Birks, H.J.B., Bjune, A.E., Birks, H.H., Solhøy, T., 2010. Oribatid mite assemblages across the tree-line in western Norway and their representation in lake sediments. J. Paleolimnol. 44, 361–374. https://doi.org/10.1007/s10933-010-9411-y.

Duprat-Oualid, F., 2019. 50 000 ans d'histoire de la végétation et du climat en Europe occidentale : étude pollinique et approche multi-proxy sur la séquence sédimentaire du Bergsee (Forêt Noire, Allemagne). PhD thesis. Université Bourgogne Franche-Comté. France. Available at: https://theses.hal.science/tel-02338676/.

Duprat-Oualid, F., Rius, D., Bégeot, C., Magny, M., Millet, L., Wulf, S., Appelt, O., 2017. Vegetation response to abrupt climate changes in Western Europe from 45 to 14.7k cal a BP - the Bergsee lacustrine record (Black Forest, Germany). J. Quat. Sci. 32, 1008–1021. https://doi.org/10.1002/jqs.2972.

Ehlers, J., Gibbard, P.L., Hughes, P.D., 2011. Quaternary Glaciations - Extent and Chronology. Elsevier, Amsterdam, p. 1108p.

Eggermont, H., Heiri, O., 2012. The chironomid-temperature relationship: expression in nature and palaeoenvironmental implications. Biol. Rev. 87, 430–456. https://doi.org/10.1111/j.1469-185X.2011.00206.x.

Eggermont, H., Heiri, O., Russell, J., Vuille, M., Audenaert, L., Verschuren, D., 2010. Paleotemperature reconstruction in tropical Africa using fossil Chironomidae (Insecta: Diptera). J. Paleolimnol. 43, 413–435. https://doi.org/10.1007/s10933-009-9339-2.

Engels, S., Bohncke, S.J.P., Bos, J.A.A., Brooks, S.J., Heiri, O., Helmens, K.F., 2008. Chironomid-based palaeotemperature estimates for northeast Finland during oxygen isotope stage 3. J. Paleolimnol. 40, 49–61. https://doi.org/10.1007/s10933-007-9133-y.

Engels, S., Helmens, K.F., Väliranta, M., Brooks, S.J., Birks, H.J.B., 2010. Early Weichselian (MIS 5d and 5c) temperatures and environmental changes in northern Fennoscandia as recorded by chironomids and macroremains at Sokli, northeast Finland. Boreas 39, 689–704. https://doi.org/10.1111/j.1502-3885.2010.00163.x.

Engels, S., Medeiros, A.S., Axford, Y., Brooks, S.J., Heiri, O., Luoto, T.P., Nazarova, L., Porinchu, D.F., Quinlan, R., Self, A.E., 2020. Temperature change as a driver of spatial patterns and long-term trends in chironomid (Insecta: Diptera) diversity. Global Change Biol. 26, 1155–1169. https://doi.org/10.1111/gcb.14862.

Fletcher, W.J., Sánchez Goñi, M.F., Allen, J.R.M., Cheddadi, R., Combourieu-Nebout, N., Huntley, B., Lawson, I., Londeix, L., Magri, D., Margari, V., Müller, U.C., Naughton, F., Novenko, E., Roucoux, K., Tzedakis, P.C., 2010. Millennial-scale variability during the last glacial in vegetation records from Europe. Quat. Sci. Rev. 29, 2839–2864. https://doi.org/10.1016/j.quascirev.2009.11.015.

Galbraith, E.D., Skinner, L.C., 2020. The biological pump during the last glacial maximum. Ann. Rev. Mar. Sci 12, 559–586. https://doi.org/10.1146/annurev-marine-010419-010906.

Gannon, J.E., 1971. Two counting cells for the enumeration of zooplankton micro-Crustacea. Trans. Am. Microsc. 90, 486. https://doi.org/10.2307/3225467.

Geyer, O.F., Schober, T., Geyer, M., 2003. Die Hochrhein-Region zwischen Bodensee und Basel. Gebrüder Borntraeger Verlagsbuchhandlung, Berlin & Stuttgart (Borntraeger), p. 526p. Stuttgart.

Grimm, E.C., 1987. CONISS: a FORTRAN 77 program for stratigraphically constrained cluster analysis by the method of incremental sum of squares. Comput. Geosci. 13, 13–35. https://doi.org/10.1016/0098-3004(87)90022-7.

Grootes, P.M., Stuiver, M., White, J.W.C., Johnsen, S., Jouzel, J., 1993. Comparison of oxygen isotope records from the GISP2 and GRIP Greenland ice cores. Nature 366, 552–554. https://doi.org/10.1038/366552a0.

Guiot, J., Pons, A., De Beaulieu, J.L., Reille, M., 1989. A 140,000-year continental climate reconstruction from two European pollen records. Nature 338, 309–313. https://doi.org/10.1038/338309a0.

Guiot, J., De Beaulieu, J.L., Cheddadi, R., David, F., Ponel, P., Reille, M., 1993. The climate in Western Europe during the last Glacial/Interglacial cycle derived from pollen and insect remains. Palaeogeogr. Palaeoclimatol. Palaeoecol. 103, 73–93. https://doi.org/10.1016/0031-0182(93)90053-L.

Haas, J.N., 1994. First identification key for charophyte oospores from central Europe. Eur. J. Phycol. 29, 227–235. https://doi.org/10.1080/09670269400650681.

Harrison, S.P., Sanchez Goñi, M.F., 2010. Global patterns of vegetation response to millennial-scale variability and rapid climate change during the last glacial period. Quat. Sci. Rev. 29, 2957–2980. https://doi.org/10.1016/j.quascirev.2010.07.016.

Heiri, O., 2004. Within-lake variability of subfossil chironomid assemblages in shallow Norwegian lakes. J. Paleolimnol. 32, 67–84. https://doi.org/10.1023/B:JOPL.0000025289.30038.e9.

Heiri, O., Brooks, S.J., Birks, H.J.B., Lotter, A.F., 2011. A 274-lake calibration data-set and inference model for chironomid-based summer air temperature reconstruction in Europe. Quat. Sci. Rev. 30, 3445–3456. https://doi.org/10.1016/j.quascirev.2011.09.006.

Heiri, O., Cremer, H., Engels, S., Hoek, W.Z., Peeters, W., Lotter, A.F., 2007. Lateglacial summer temperatures in the Northwest European lowlands: a chironomid record from Hijkermeer, The Netherlands. Quat. Sci. Rev. 26, 2420–2437. https://doi.org/10.1016/j.quascirev.2007.06.017.

Heiri, O., Lotter, A.F., 2001. Effect of low count sums on quantitative environmental reconstructions: an example using subfossil chironomids. J. Paleolimnol. 26, 343–350. https://doi.org/10.1023/A:1017568913302.

Heiri, O., Lotter, A.F., Hausmann, S., Kienast, F., 2003. A chironomid-based Holocene summer air temperature reconstruction from the Swiss Alps. Holocene 13, 477–484. https://doi.org/10.1191/0959683603hl640ft.

Heiri, O., Lotter, A.F., 2005. Holocene and Lateglacial summer temperature reconstruction in the Swiss Alps based on fossil assemblages of aquatic organisms - a review. Boreas 34, 506–516. https://doi.org/10.1080/03009480500231229.

Heiri, O., Millet, L., 2005. Reconstruction of late glacial summer temperatures from chironomid assemblages in lac Lautrey (Jura, France). J. Quat. Sci. 20, 33–44. https://doi.org/10.1002/jqs.895.

Heiri, O., Koinig, K.A., Spötl, C., Barrett, S., Brauer, A., Drescher-Schneider, R., Gaar, D., Ivy-Ochs, S., Kerschner, H., Luetscher, M., Moran, A., Nicolussi, K., Preusser, F., Schmidt, R., Schoeneich, P., Schwörer, C., Sprafke, T., Terhorst, B., Tinner, W., 2014. Palaeoclimate records 60–8 ka in the Austrian and Swiss Alps and their forelands. Quat. Sci. Rev. 106, 186–205. https://doi.org/10.1016/j.quascirev.2014.05.021.

Heiri, O., Ilyashuk, B., Millet, L., Samartin, S., Lotter, A.F., 2015. Stacking of discontinuous regional palaeoclimate records: chironomid-based summer temperatures from the Alpine region. Holocene 25, 137–149. https://doi.org/10.1177/0959683614556382.

Hemmerle, H., May, J.-H., Preusser, F., 2016. Übersicht über die pleistozänen Vergletscherungen des Schwarzwaldes. Ber. Naturf. Ges. Freiburg i. Br. 106, 31–67.

Hofmann, F.M., Preusser, F., Schimmelpfennig, I., Léanni, L., Team, Aster, Aumaître, Georges, Karim, Keddadouche, Fawzi, Zaid, 2022. Late Pleistocene glaciation history of the southern Black Forest, Germany: ^{10}Be cosmic-ray exposure dating and equilibrium line altitude reconstructions in Sankt Wilhelmer Tal. J. Quat. Sci. 37, 688–706. https://doi.org/10.1002/jqs.3407.

Hofmann, F.M., Rauscher, F., McCreary, W., Bischoff, J.-P., Preusser, F., 2020. Revisiting late Pleistocene glacier dynamics north-west of the feldberg, southern Black forest, Germany. EGQSJ 69, 61–87. https://doi.org/10.5194/egqsj-69-61-2020.

Hofmann, F.M., 2023. Geometry, chronology and dynamics of the last Pleistocene glaciation of the Black Forest. E&G Quaternary Sci. J. 72, 235–237. https://doi.org/10.5194/egqsj-72-235-2023.

Hofmann, W., 2001. Late-Glacial/Holocene succession of the chironomid and cladoceran fauna of the Soppensee (Central Switzerland). J. Paleolimnol. 25, 411–420. https://doi.org/10.1023/A:1011103820283.

Hughes, P.D., Gibbard, P.L., Ehlers, J., 2013. Timing of glaciation during the last glacial cycle: evaluating the concept of a global 'Last Glacial Maximum' (LGM). Earth Sci. Rev. 125, 171–198. https://doi.org/10.1016/j.earscirev.2013.07.003.

Ilyashuk, E.A., Ilyashuk, B.P., Heiri, O., Spötl, C., 2022. Summer temperatures and environmental dynamics during the middle würmian (MIS 3) in the eastern Alps: multi-proxy records from the Unterangerberg palaeolake, Austria. Quat. Sci. Adv. 6, 100050. https://doi.org/10.1016/j.qsa.2022.100050.

Ivy-Ochs, S., Kerschner, H., Reuther, A., Preusser, F., Heine, K., Maisch, M., Kubik, P.W., Schlüchter, C., 2008. Chronology of the last glacial cycle in the European Alps. J. Quat. Sci. 23, 559–573. https://doi.org/10.1002/jqs.1202.

Ivy-Ochs, S., 2015. Glacier variations in the European Alps at the end of the last glaciation. Cuadernos Invest. Geogr. 41, 295–315. https://doi.org/10.18172/cig.2750.

Ivy-Ochs, S., Schäfer, J., Kubik, P.W., Synal, H.-A., Schlüchter, C., 2004. Timing of deglaciation on the northern Alpine foreland (Switzerland). Eclogae Geol. Helv. 97, 47–55. https://doi.org/10.1007/s00015-004-1110-0.

Janecek, B., Moog, O., Orendt, C., 2017. Diptera: chironomidae (Non-Biting midges). In: Fauna Aquatica Austriaca, p. 111p. Wien, Austria.

Juggins, S., 2017. C2: Software for Ecological and Palaeoecological Data Analysis and Visualisation Version 1.7.7. Newcastle University, Newcastle upon Tyne, p. 77p.

Juggins, S., 2023. Rioja: analysis of quaternary science data. R package version 1.0–6. https://cran.r-project.org/package=rioja.

Kamleitner, S., Ivy-Ochs, S., Manatschal, L., Akçar, N., Christl, M., Vockenhuber, C., Hajdas, I., Synal, H.-A., 2023. Last Glacial Maximum glacier fluctuations on the northern Alpine foreland: geomorphological and chronological reconstructions from the Rhine and Reuss glacier systems. Geomorphology 423, 108548. https://doi.org/10.1016/j.geomorph.2022.108548.

Kämpf, L., Rius, D., Duprat-Oualid, F., Crouzet, C., Millet, L., 2022. Evidence for wind patterns and associated landscape response in Western Europe between 46 and 16 cal ka BP. Quat. Sci. Rev. 298, 107846. https://doi.org/10.1016/j.quascirev.2022.107846.

Kim, S.-J., Flato, G., Boer, G., 2003. A coupled climate model simulation of the Last Glacial Maximum, Part 2: approach to equilibrium. Clim. Dynam. 20, 635–661. https://doi.org/10.1007/s00382-002-0292-2.

Landolt, E., Aeschimann, D., Bäumler, B., Rasolofo, N., 2015. Unsere Alpenflora: ein Pflanzenführer für Wanderer und Bergsteiger. Schweizer Alpen-Club SAC, Switzerland, p. 488p.

Larocque, I., 2001. How many chironomid head capsules are enough? A statistical approach to determine sample size for palaeoclimatic reconstructions. Palaeogeogr. Palaeoclimatol. Palaeoecol. 172, 133–142. https://doi.org/10.1016/S0031-0182(01)00278-4.

Larocque-Tobler, I., Heiri, O., Wehrli, M., 2010. Late Glacial and Holocene temperature changes at Egelsee, Switzerland, reconstructed using subfossil chironomids. J. Paleolimnol. 43, 649–666. https://doi.org/10.1007/s10933-009-9358-z.

Laskar, J., Robutel, P., Joutel, F., Gastineau, M., Correia, A.C.M., Levrard, B., 2004. A long-term numerical solution for the insolation quantities of the Earth. Astron. Astrophys. 428, 261–285. https://doi.org/10.1051/0004-6361:20041335.

Lemdahl, G., 2000. Lateglacial and Early Holocene insect assemblages from sites at different altitudes in the Swiss Alps—implications on climate and environment. Palaeogeogr. Palaeoclimatol. Palaeoecol. 159, 293–312. https://doi.org/10.1016/S0031-0182(00)00091-2.

Lisiecki, L.E., Raymo, M.E., 2005. A Pliocene-Pleistocene stack of 57 globally distributed benthic δ^{18}O records. Paleoceanography 20. https://doi.org/10.1029/2004PA001071, 2004PA001071.

Livingstone, D.M., Lotter, A.F., Walkery, I.R., 1999. The decrease in summer surface water temperature with altitude in Swiss alpine lakes: a comparison with air temperature lapse rates. Arctic Antarct. Alpine Res. 31, 341–352. https://doi.org/10.1080/15230430.1999.12003319.

Lods-Crozet, B., Lachavanne, J.-B., 1994. Changes in the chironomid communities in Lake Geneva in relation with eutrophication, over a period of 60 years. Arch. Hydrobiol. 130, 453–471. https://doi.org/10.1127/archiv-hydrobiol/130/1994/453.

Lotter, A.F., Heiri, O., Brooks, S., van Leeuwen, J.F.N., Eicher, U., Ammann, B., 2012. Rapid summer temperature changes during Termination 1a: high-resolution multi-proxy climate reconstructions from Gerzensee (Switzerland). Quat. Sci. Rev. 36, 103–113. https://doi.org/10.1016/j.quascirev.2010.06.022.

Luetscher, M., Boch, R., Sodemann, H., Spötl, C., Cheng, H., Edwards, R.L., Frisia, S., Hof, F., Müller, W., 2015. North atlantic storm track changes during the last glacial maximum recorded by alpine speleothems. Nat. Commun. 6, 6344. https://doi.org/10.1038/ncomms7344.

Luoto, T.P., 2009. Subfossil Chironomidae (Insecta: Diptera) along a latitudinal gradient in Finland: development of a new temperature inference model. J. Quat. Sci. 24, 150–158. https://doi.org/10.1002/jqs.1191.

Luoto, T.P., Nevalainen, L., 2009. Larval chaoborid mandibles in surface sediments of small shallow lakes in Finland: implications for palaeolimnology. Hydrobiologia 631, 185–195. https://doi.org/10.1007/s10750-009-9810-0.

Luoto, T.P., Kaukolehto, M., Weckström, J., Korhola, A., Väliranta, M., 2014. New evidence of warm early-Holocene summers in subarctic Finland based on an enhanced regional chironomid-based temperature calibration model. Quat. Res. 81, 50–62. https://doi.org/10.1016/j.yqres.2013.09.010.

Martrat, B., Grimalt, J.O., Lopez-Martinez, C., Cacho, I., Sierro, F.J., Flores, J.A., Zahn, R., Canals, M., Curtis, J.H., Hodell, D.A., 2004. Abrupt temperature changes in the western mediterranean over the past 250,000 years. Science 306, 1762–1765. https://doi.org/10.1126/science.1101706.

Massicotte, P., South, A., 2023. Rnaturalearth: world map data from natural earth. R package version 1.0.1. https://CRAN.R-project.org/package=rnaturalearth.

Mercier, J.-L., Jeser, N., 2004. The glacial history of the Vosges Mountains. In: Ehlers, J., Gibbard, P.L. (Eds.), Developments in Quaternary Sciences. Elsevier, pp. 113–118. https://doi.org/10.1016/S1571-0866(04)80061-7.

Millet, L., Rius, D., Galop, D., Heiri, O., Brooks, S.J., 2012. Chironomid-based reconstruction of Lateglacial summer temperatures from the Ech palaeolake record (French western Pyrenees). Palaeogeogr. Palaeoclimatol. Palaeoecol. 315–316, 86–99. https://doi.org/10.1016/j.palaeo.2011.11.014.

Moller Pillot, H.K.M., 2013. Biology and Ecology of Aquatic Orthocladiinae. KNNV Publishing, Zeist, The Netherlands, p. 312p.

Monegato, G., Ravazzi, C., Donegana, M., Pini, R., Calderoni, G., Wick, L., 2007. Evidence of a two-fold glacial advance during the last glacial maximum in the Tagliamento end moraine system (eastern Alps). Quat. Res. 68, 284–302. https://doi.org/10.1016/j.yqres.2007.07.002.

Monegato, G., Scardia, G., Hajdas, I., Rizzini, F., Piccin, A., 2017. The Alpine LGM in the boreal ice-sheets game. Sci. Rep. 7, 2078. https://doi.org/10.1038/s41598-017-02148-7.

Moseley, G.E., Spötl, C., Brandstätter, S., Erhardt, T., Luetscher, M., Edwards, R.L., 2020. NALPS19: sub-orbital-scale climate variability recorded in northern Alpine speleothems during the last glacial period. Clim. Past 16, 29–50. https://doi.org/10.5194/cp-16-29-2020.

Müller, P.C., 1994. Die Hotzenwälder Wuhren : ein Beitrag zur Wirtschaftsgeschichte des Hochrheins. Vom Jura zum Schwarzwald : Blätter für Heimatkunde und Heimatschutz 68, 85–97. https://doi.org/10.5169/SEALS-747181.

Müller, U.C., Pross, J., Bibus, E., 2003. Vegetation response to rapid climate change in Central Europe during the past 140,000 yr based on evidence from the Füramoos pollen record. Quat. Res. 59, 235–245. https://doi.org/10.1016/S0033-5894(03)00005-X.

Nazarova, L., Self, A.E., Brooks, S.J., van Hardenbroek, M., Herzschuh, U., Diekmann, B., 2015. Northern Russian chironomid-based modern summer temperature data set and inference models. Global Planet. Change 134, 10–25. https://doi.org/10.1016/j.gloplacha.2014.11.015.

Oksanen, J., Simpson, G.L., Guillaume Blanchet, F., Kindt, R., Legendre, P., Minchin, P. R., O'Hara, R.B., Solymos, P., Henry, M., Stevens, H., Szoecs, E., Wagner, H., Barbour, M., Bedward, M., Bolker, B., Borcard, D., Carvalho, G., Chirico, M., De Caceres, M., Durand, S., Beatriz Antoniazi Evangelista, H., FitzJohn, R., Friendly, M., Furneaux, B., Hannigan, G., Hill, M.O., Lahti, L., McGlinn, D., Ouellette, M.-H., Ribeiro Cunha, E., Smith, T., Stier, A., ter Braak, C.J.F., Weedon, J., 2022. Vegan: community ecology package. R package version 2.6–4. https://CRAN.R-project.org/package=vegan.

Perret-Gentil, N., Rey, F., Gobet, E., Tinner, W., Heiri, O., 2023. Human impact leads to unexpected oligotrophication and deepwater oxygen increase in a Swiss mountain lake. Holocene 34, 189–201. https://doi.org/10.1177/09596836231211821.

Pini, R., Ravazzi, C., Reimer, P.J., 2010. The vegetation and climate history of the last glacial cycle in a new pollen record from Lake Fimon (southern Alpine foreland, N-Italy). Quat. Sci. Rev. 29, 3115–3137. https://doi.org/10.1016/j.quascirev.2010.06.040.

Preusser, F., Graf, H.R., Keller, O., Krayss, E., Schlüchter, C., 2011. Quaternary glaciation history of northern Switzerland. E&G Quaternary Sci. J. 60, 282–305. https://doi.org/10.3285/eg.60.2-3.06.

Quinlan, R., Smol, J.P., 2001a. Setting minimum head capsule abundance and taxa deletion criteria in chironomid-based inference models. J. Paleolimnol. 26, 327–342. https://doi.org/10.1023/A:1017546821591.

Quinlan, R., Smol, J.P., 2001b. Chironomid-based inference models for estimating end-of-summer hypolimnetic oxygen from south-central Ontario shield lakes. Freshw. Biol. 46, 1529–1551. https://doi.org/10.1046/j.1365-2427.2001.00763.x.

Quinlan, R., Smol, J.P., 2010. Use of subfossil *Chaoborus* mandibles in models for inferring past hypolimnetic oxygen. J. Paleolimnol. 44, 43–50. https://doi.org/10.1007/s10933-009-9384-x.

R Core Team, 2022. R: A Language and Environment for Statistical Computing. R Foundation for Statistical Computing, Vienna, Austria. https://www.r-project.org.

Rasmussen, S.O., Bigler, M., Blockley, S.P., Blunier, T., Buchardt, S.L., Clausen, H.B., Cvijanovic, I., Dahl-Jensen, D., Johnsen, S.J., Fischer, H., Gkinis, V., Guillevic, M., Hoek, W.Z., Lowe, J.J., Pedro, J.B., Popp, T., Seierstad, I.K., Steffensen, J.P., Svensson, A.M., Vallelonga, P., Vinther, B.M., Walker, M.J.C., Wheatley, J.J., Winstrup, M., 2014. A stratigraphic framework for abrupt climatic changes during the Last Glacial period based on three synchronized Greenland ice-core records: refining and extending the INTIMATE event stratigraphy. Quat. Sci. Rev. 106, 14–28. https://doi.org/10.1016/j.quascirev.2014.09.007.

Reede, T., 1995. Life history shifts in response to different levels of fish kairomones in *Daphnia*. J. Plankton Res. 17, 1661–1667. https://doi.org/10.1093/plankt/17.8.1661.

Reimer, P.J., Austin, W.E.N., Bard, E., Bayliss, A., Blackwell, P.G., Bronk Ramsey, C., Butzin, M., Cheng, H., Edwards, R.L., Friedrich, M., Grootes, P.M., Guilderson, T.P., Hajdas, I., Heaton, T.J., Hogg, A.G., Hughen, K.A., Kromer, B., Manning, S.W., Muscheler, R., Palmer, J.G., Pearson, C., van der Plicht, J., Reimer, R.W., Richards, D.A., Scott, E.M., Southon, J.R., Turney, C.S.M., Wacker, L., Adolphi, F., Büntgen, U., Capano, M., Fahrni, S.M., Fogtmann-Schulz, A., Friedrich, R., Köhler, P., Kudsk, S., Miyake, F., Olsen, J., Reinig, F., Sakamoto, M., Sookdeo, A., Talamo, S., 2020. The IntCal20 northern hemisphere Radiocarbon age calibration curve (0–55 cal kBP). Radiocarbon 62, 725–757. https://doi.org/10.1017/RDC.2020.41.

Reiss, F., Gerstmeier, R., 1984. *Corynocera ambigua* Zetterstedt als Glazialrelikt im Starnberger See, Oberbayern (Diptera, Chironomidae). Nach.bl. bayer. Entomol. 33, 58–61.

Rey, F., Gobet, E., van Leeuwen, J.F.N., Gilli, A., van Raden, U.J., Hafner, A., Wey, O., Rhiner, J., Schmocker, D., Zünd, J., Tinner, W., 2017. Vegetational and agricultural dynamics at Burgäschisee (Swiss Plateau) recorded for 18,700 years by multi-proxy evidence from partly varved sediments. Veget. Hist. Archeobot. 26, 571–586. https://doi.org/10.1007/s00334-017-0635-x.

Rey, F., Gobet, E., Schwörer, C., Hafner, A., Szidat, S., Tinner, W., 2020. Climate impacts on vegetation and fire dynamics since the last deglaciation at Moossee (Switzerland). Clim. Past 16, 1347–1367. https://doi.org/10.5194/cp-16-1347-2020.

Russo, E., Buzan, J., Lienert, S., Jouvet, G., Velasquez Alvarez, P., Davis, B., Ludwig, P., Joos, F., Raible, C., 2024. High resolution LGM climate over Europe and the Alpine region using the regional climate model WRF. Clim. Past 20, 449–465. https://doi.org/10.5194/cp-20-449-2024.

Sæther, O.A., 1979. Chironomid communities as water quality indicators. Holarct. Ecol. 2, 65–74. https://doi.org/10.1111/j.1600-0587.1979.tb00683.x.

Salmela, J., Härmä, O., Taylor, D.J., 2021. *Chaoborus flavicans* Meigen (Diptera, Chaoboridae) is a complex of lake and pond dwelling species: a revision. Zootaxa 4927 (2), 151–196. https://doi.org/10.11646/zootaxa.4927.2.1.

Samartin, S., Heiri, O., Lotter, A.F., Tinner, W., 2012. Climate warming and vegetation response after Heinrich event 1 (16 700–16 000 cal yr BP) in Europe south of the Alps. Clim. Past 8, 1913–1927. https://doi.org/10.5194/cp-8-1913-2012.

Samartin, S., Heiri, O., Kaltenrieder, P., Kühl, N., Tinner, W., 2016. Reconstruction of full glacial environments and summer temperatures from Lago della Costa, a refugial site in Northern Italy. Quat. Sci. Rev. 143, 107–119. https://doi.org/10.1016/j.quascirev.2016.04.005.

Sánchez Goñi, M.F., Landais, A., Fletcher, W.J., Naughton, F., Desprat, S., Duprat, J., 2008. Contrasting impacts of Dansgaard–Oeschger events over a western European latitudinal transect modulated by orbital parameters. Quat. Sci. Rev. 27, 1136–1151. https://doi.org/10.1016/j.quascirev.2008.03.003.

Schmid, P.E., 1993. A key to the larval chironomidae and their instars from Austrian danube region streams and rivers. In: Federal Institute for Water Quality, vol. 514p. Wien, Austria.

Shackleton, N.J., Sánchez-Goñi, M.F., Pailler, D., Lancelot, Y., 2003. Marine Isotope Substage 5e and the Eemian Interglacial. Global Planet. Change 36, 151–155. https://doi.org/10.1016/S0921-8181(02)00181-9.

Shakun, J.D., Carlson, A.E., 2010. A global perspective on Last Glacial Maximum to Holocene climate change. Quat. Sci. Rev. 29, 1801–1816. https://doi.org/10.1016/j.quascirev.2010.03.016.

Šmilauer, P., Lepš, J., 2014. Multivariate Analysis of Ecological Data Using CANOCO 5, vol. 362p. Cambridge University Press. https://doi.org/10.1017/CBO9781139627061.

Solhøy, I.W., Solhøy, T., 2000. The fossil oribatid mite fauna (Acari: Oribatida) in late-glacial and early-Holocene sediments in Kråkenes Lake, western Norway. J. Paleolimnol. 23, 35–47. https://doi.org/10.1023/A:1008068915118.

Solhøy, T., 2001. Oribatid mites. In: Smol, J.P., Birks, H.J.B., Last, W.M. (Eds.), Tracking Environmental Change Using Lake Sediments: Volume 4 Zoological Indicators. Kluwer Academic Publishers, Dordrecht, pp. 81–104.

Spötl, C., Koltai, G., Jarosch, A.H., Cheng, H., 2021. Increased autumn and winter precipitation during the last glacial maximum in the European Alps. Nat. Commun. 12, 1839. https://doi.org/10.1038/s41467-021-22090-7.

Stötter, T., 2015. In: Methane-derived Carbon in Recent and Ancient Lake Sediments – Analyses of Lipids and Invertebrate Remains. University of Bern, Switzerland. PhD thesis.

Strandberg, G., Brandefelt, J., Kjellström, E., Smith, B., 2011. High-resolution regional simulation of last glacial maximum climate in Europe. Tellus 63, 107. https://doi.org/10.1111/j.1600-0870.2010.00485.x.

Sweetman, J.N., Smol, J.P., 2006. Reconstructing fish populations using *Chaoborus* (Diptera: chaoboridae) remains – a review. Quat. Sci. Rev. 25, 2013–2023. https://doi.org/10.1016/j.quascirev.2006.01.007.

Szeroczyńska, K., Sarmaja-Korjonen, K., 2007. Atlas of Subfossil Cladocera from Central and Northern Europe. Friends of the Lower Vistula Society, Poland, p. 83p.

Tarkowska-Kukuryk, M., 2014. Spatial distribution of epiphytic chironomid larvae in a shallow macrophyte-dominated lake: effect of macrophyte species and food resources. Limnology 15, 141–153. https://doi.org/10.1007/s10201-014-0425-4.

ter Braak, C.J.F., 1995. Non-linear methods for multivariate statistical calibration and their use in palaeoecology: a comparison of inverse (k-nearest neighbours, partial least squares and weighted averaging partial least squares) and classical approaches. Chemom. Intell Lab Syst 28, 165–180. https://doi.org/10.1016/0169-7439(95)80048-E.

ter Braak, C.J.F., Juggins, S., Birks, H.J.B., Van der Voet, H., 1993. Weighted averaging partial least squares regression (WA-PLS): definition and comparision with other methods for species-environment calibration, in: patil, G.P., rao, C.R. (eds.), multivariate environmental statistics. Elsevier science publishers, amsterdam. The Netherlands 525–560.

Tóth, M., Magyari, E.K., Brooks, S.J., Braun, M., Buczkó, K., Bálint, M., Heiri, O., 2012. A chironomid-based reconstruction of late glacial summer temperatures in the southern Carpathians (Romania). Quat. Res. 77, 122–131. https://doi.org/10.1016/j.yqres.2011.09.005.

Ursenbacher, S., Stötter, T., Heiri, O., 2020. Chitinous aquatic invertebrate assemblages in Quaternary lake sediments as indicators of past deepwater oxygen concentration. Quat. Sci. Rev. 231, 106203. https://doi.org/10.1016/j.quascirev.2020.106203.

Uutala, A.J., 1990. *Chaoborus* (Diptera: chaoboridae) mandibles-paleolimnological indicators of the historical status of fish populations in acid-sensitive lakes. J. Paleolimnol. 4. https://doi.org/10.1007/BF00226321.

Vandekerkhove, J., Declerck, S., Vanhove, M., Brendonck, L., Jeppesen, E., Conde Porcuna, J.M., De Meester, L., 2004. Use of ephippial morphology to assess richness of anomopods: potentials and pitfalls. J. Limnol. 63, 75. https://doi.org/10.4081/jlimnol.2004.s1.75.

Velle, G., Brodersen, K.P., Birks, H.J.B., Willassen, E., 2010. Midges as quantitative temperature indicator species: lessons for palaeoecology. Holocene 20, 989–1002. https://doi.org/10.1177/0959683610365933.

von Gunten, L., Heiri, O., Bigler, C., Van Leeuwen, J., Casty, C., Lotter, A.F., Sturm, M., 2008. Seasonal temperatures for the past ~400 years reconstructed from diatom and chironomid assemblages in a high-altitude lake (Lej da la Tscheppa, Switzerland). J. Paleolimnol. 39, 283–299. https://doi.org/10.1007/s10933-007-9103-4.

Walker, I.R., Levesque, A.J., Cwynar, L.C., Lotter, A.F., 1997. An expanded surface-water palaeotemperature inference model for use with fossil midges from eastern Canada. J. Paleolimnol. 18, 165–178. https://doi.org/10.1023/A:1007997602935.

Walker, I.R., Smol, J.P., Engstrom, D.R., Birks, H.J.B., 1991. An assessment of chironomidae as quantitative indicators of past climatic change. Can. J. Fish. Aquat. Sci. 48, 975–987. https://doi.org/10.1139/f91-114.

Wiederholm, T., 1983. Chironomidae of the holarctic region. Keys and diagnoses. Part 1. Larvae. Entomologica scandinavica. Motala 457p.

Wood, T.S., Okamura, B., 2005. A new key to the freshwater bryozoans of Britain, Ireland and continental Europe, with notes on their ecology. Freshwater Biological Association. Ambleside 113p.

Wütrich, C., Leser, H., 2000. Bergsee bad säckingen. Die limnoökologische situation 1998-2000. Department Geographie der Universität Basek, Abteilung Physiogeographie und Landschaftsökologie, p. 25.

Zander, P.D., Böhl, D., Sirocko, F., Auderset, A., Haug, G.H., Martínez-García, A., 2024. Reconstruction of warm-season temperatures in central Europe during the past 60 000 years from lacustrine branched glycerol dialkyl glycerol tetraethers (brGDGTs). Clim. Past 20, 841–864. https://doi.org/10.5194/cp-20-841-2024.